Economic Geology
Vol. 85, 1990, pp. 50–75

Geology and Geochemistry of the Vantage Gold Deposits, Alligator Ridge-Bald Mountain Mining District, Nevada

R. P. ILCHIK*

Department of Earth and Space Sciences, University of California, Los Angeles, Los Angeles, California 90024

Abstract

Geologic relationships, major element data, and isotopic geochemistry of a group of Carlin-type Au deposits in the Alligator Ridge-Bald Mountain district of east-central Nevada were investigated to help constrain the origin and relative timing of Au mineralization and associated alteration. The Vantage gold deposits were the largest of 18 known sediment-hosted, disseminated gold deposits and prospects that are distributed over a strike length of 40 km. The district consists predominantly of Paleozoic carbonate and siliciclastic sedimentary rocks. Minor amounts of Tertiary volcanic and volcanic-related sedimentary rocks and a small granitic stock in the northern end of the district are also present. The intrusion and its surrounding aureole also host gold mineralization, but most gold deposits in the district are not spatially associated with intrusive rocks.

The Vantage Au deposits formed at the contact between the Devonian Devils Gate Limestone and the Devonian-Mississippian Pilot Shale adjacent to a major fault zone, herein referred to as the Vantage fault. Gold mineralization was accompanied by silver, antimony, and arsenic and showed a strong preference for the Pilot Shale. Alteration related in time and space to Au mineralization was the replacement of host-rock carbonates by quartz. Replacement in the Pilot Shale closely followed the ore-waste boundary, whereas replacement in the Devils Gate Limestone occurred as a stratiform jasperoid not confined to the ore zones. Quartz + kaolinite + stibnite veins were common within the central, high-grade portion of each orebody. Peripheral to silicification, diagenetic dolomite in the Pilot Shale was replaced by hydrothermal calcite, and calcite veins constituted as much as 10 percent of the rocks. Two oxidation events that destroyed organic matter and sulfides occurred after Au deposition and silicification. The early oxidation event was accompanied by the destruction of detrital illite in the Pilot Shale and deposition of alunite ± barite veins. This event was barren of Au but did redistribute metals introduced during silicification. The spatial distribution of this alteration was similar to that of the silicification. K-Ar dating of this alunite indicates an age of 11 Ma for its formation. Following a period of erosion, weathering-related oxidation overprinted much of the earlier alteration and deposited jarosite and goethite, but it did not affect metal distribution patterns or the matrix of the Pilot Shale.

Whole-rock chemical analyses indicate that silica and sulfur were the only major components introduced during silicification and that very little material other than iron and organic matter was removed during the intense oxidation. Oxygen isotope compositions determined for jasperoid and vein quartz varied from 15.9 to 18.2 per mil, and from 16.1 to 20.1 per mil, respectively. Carbonate from whole-rock samples peripheral to silicification showed an increase in their carbon isotope values of up to 3 per mil (to 1.4‰) and a decrease in their oxygen isotope values of up to 12 per mil (to 12.7‰) in comparison with unaltered samples. Vein calcite had even more extreme values of up to 3.1 per mil for $\delta^{13}C$ and 3.8 per mil for $\delta^{18}O$. Sulfur isotope measurements on stibnite and orpiment varied from 5.5 to 10 per mil and from 2.5 to 12.3 per mil, respectively. Vein alunite and barite associated with intense oxidation had sulfur isotope compositions that generally varied from 3.8 to 13.4 per mil, and from 21.0 to 29.2 per mil, respectively. Barite that appeared to be sedimentary in origin yielded values of 25.9 to 47.1 per mil.

Hydrothermal fluids that formed the deposits ascended from depth along the Vantage fault. Near the level of the deposits, fluids were displaced into minor faults in the footwall limestone. At the contact between the Devils Gate Limestone and the Pilot Shale, fluids spread laterally and deposited Au, Ag, Sb, and As and quartz. Following Au deposition, hypogene oxidizing fluids using the same conduits destroyed reduced components in the Pilot Shale and produced major textural modifications. The distribution of the elements within the deposits appears to be related to (1) proximity to hydrothermal conduits, (2) composition of the host lithologies, and (3) extent of postmineralization oxidation. Oxygen isotope data of jasperoid and vein quartz indicate that the ore fluids were evolved meteoric waters. Isotopic data for epigenetic sulfides indicate that sulfur was derived from sedimentary sulfides; local stratigraphic consid-

* Present address: Department of Geosciences, University of Arizona, Tuscon, Arizona 85721.

0361-0128/90/1031/50-26$3.00

erations suggest that Cambrian siliciclastic rocks were the source. The deposits were geochemically similar to other sediment-hosted gold deposits in the Great Basin (e.g., Carlin), but they were uncomplicated by extraneous geologic features such as Paleozoic thrusts or premineralization intrusions. Thus, the Vantage deposits may be more easily understood examples of this class of ore deposits.

Introduction

THE discovery of the Carlin sediment-hosted gold deposit in the Lynn district coupled with the dramatic increase in gold prices in the 1970s renewed gold exploration in the Basin and Range province. This region is currently one of the largest producers of gold in the world (Thomas and Boyle, 1986) and continues to be the focus of intense exploration. The known sediment-hosted, disseminated Au deposits (commonly referred to as "Carlin-type") exhibit many similar characteristics (Tooker, 1985). Gold generally occurs as submicroscopic disseminations in organic-rich, silty carbonate rocks, and high concentrations of Ag, Sb, and As are also present. Gold mineralization is mainly restricted to favorable lithologies and thus is strata bound, whereas alteration reflects the paleohydrology and can be either stratiform or discordant. Wall-rock alteration most prominently associated with mineralization is removal of host-rock carbonate which is generally accompanied by deposition of quartz (i.e., jasperoid formation). Oxidation of organic matter and sulfides is commonly present, but there is no consensus on whether this oxidation is hypogene and related to other hydrothermal events, or whether it is supergene and related to erosion and weathering of the ore deposits. Available data, however, for Carlin-type deposits are insufficient to address many questions pertaining to the spatial and temporal relationships between the various alteration features, the processes of mineralization, and the regional settings of the deposits. This communication presents geological and geochemical data from the Alligator Ridge-Bald Mountain district that characterize a Carlin-type system and provide some constraints regarding genesis and regional geologic setting.

The Alligator Ridge-Bald Mountain district is a 40 km by 15 km, north-south-trending belt of mineralization located in the east-central portion of the Great Basin (Fig. 1) and includes the Bald Mountain mining district of Smith (1976). The area is located in northwestern White Pine County, Nevada, about 80 km northwest of the town of Ely and is directly south of the Ruby Mountains. The district contains 18 Au deposits and prospects (Table 1). Sixteen of these deposits are exclusively sediment-hosted and share many geochemical and geological characteristics of the Carlin-type deposits. The style of mineralization is typified by the Vantage deposits, the largest deposits yet discovered in the district. The two remaining Au deposits are found along the contact of a granitic intrusion located between Big and Little Bald Mountains. The district has experienced relatively few geologic complications unrelated to the processes of mineralization (Hose and Blake, 1976) and therefore provides an excellent opportunity to examine many of the questions regarding the geologic and geochemical environment of ore deposition in the Carlin-type systems.

Exploration and Mining History

Mining activity in the Alligator Ridge-Bald Mountain district prior to the discovery of the Vantage orebodies was very limited and restricted to the northern, Bald Mountain portion of the district (Smith, 1976). Reported production for 1869 through 1956 was 17,000 oz Ag, 125 oz Au, 15 tons Cu, and minor amounts of Sb and W, all from <900 short tons of ore. The Bald Mountain area was examined in the 1960s for porphyry copper-type mineralization and in the early 1970s for disseminated gold. Both of these exploration programs failed to locate economic mineralization. In the southern portion of the district, the only indication of prior mining activity was a picture-rock quarry for ornamental stone in Pilot Shale, 5 km south of the Vantage deposits.

Gold mineralization in the vicinity of the Vantage deposits was first indicated in 1976 by samples of jasperoid collected less than 200 m north of the Vantage I orebody (Ilchik, 1990). These samples contained up to 0.5 ppm Au. Several Vantage lode claims were subsequently located over the surrounding area. A mapping and sampling program discovered a small outcrop of the Vantage I orebody which contained up to 9 ppm Au. Soil sampling on a 500- by 200-ft grid generated a four-station anomaly in As, Sb, and Hg (up to 160 ppm, 70 ppm, and 983 ppb, respectively) as well as Au centered on this outcrop. Several other anomalies of lower intensity were found near areas of jasperoid exposure or downslope from Vantage I. Exploration drilling from late 1977 to early 1979 revealed that mineralization was confined to four pods, designated, from north to south, Vantage I to IV. Three of these areas were economic orebodies that contained combined reserves of approximately 5.8 million metric tons of ore at an average grade of 4.0 ppm, based on a 1 ppm cutoff grade. Since the initial discovery, five other mines have been developed and numerous smaller areas of mineralization discovered in the district (Fig. 1 and Table 1).

Data presented here were acquired during an 11-yr association with the exploration, development, and production of the Alligator Ridge district. The Van-

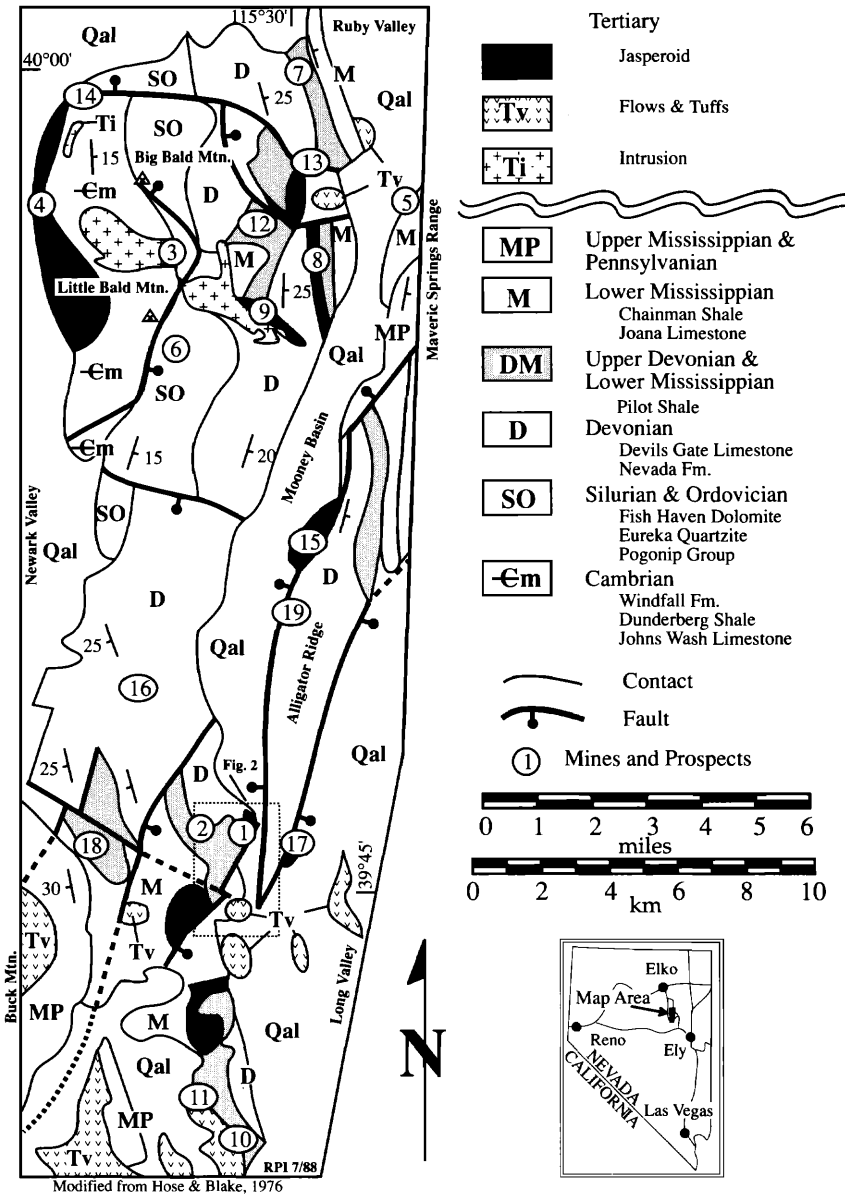

FIG. 1. Geologic map of the Alligator Ridge-Bald Mountain district showing locations of deposits, major prospects, and jasperoids. Numbers correspond to locations in Table 1.

tage basin-Luxe areas and other selected portions of the district were mapped at a scale of 1:6,000. The Vantage basin has been explored by over 800 rotary percussion drill holes and ~1,200 m of diamond core. Approximately half of the rotary holes and two-thirds of the core have been logged at scales of 1:600 and 1:48, respectively. Pit mapping was done on an intermittent basis throughout the history of the mine. The 6,400-, 6,380-, and 6,300-ft levels of Vantage II and the 6,580-ft level of Vantage III were mapped in detail at scales of 1:240 and 1:600. These levels constituted a series of exposures from the premining surface to the footwall limestone and provided a three-dimensional view of the ore deposits and adjacent areas. Mining methods, however, limited the utility of pit maps. Blasted faces were not mucked clean until the final pit walls were reached. Muck was moved up to 10 m laterally due to blast heave and thus obscured already complex alteration relationships. Diamond core provided the most reliable geologic data.

Regional Setting

The Alligator Ridge-Bald Mountain district is located in the central portion of the Great Basin. Pa-

TABLE 1. List of Mines and Prospects in the Alligator Ridge-Bald Mountain District

Mines[1]	Host rocks[2]	Type	Alteration[3]
(1) Vantage	DM	Au	S, Al, Ba
(2) Luxe	DM	Au	S
(3) Top	O, Ti	Au, Cu	S, argil., skarn
(4) Placer	Cm, O (?)	Au	S
(5) Winrock	Mj (?)	Au	S
(6) Dynasty	O	Au	S, Ba
(7) Royale	DM	Au	S, Al, Ba
Prospects[1]			
(8) Galaxy	DM	Au	S, Al, Ba
(9) Horseshoe	D, Ti	Au	S
(10) Yankee	DM	Au	S
(11) South Selox	DM	Au	S, Al, Ba
(12) Casino	DM	Au	S
(13) Duke	DM	Au	S
(14) Bald Mtn.	Cm, O	Au	S
(15) Saga	DM	Au	S
(16) Pacer	DM	Au	S, Al, Ba
(17) Gator	Mj	Au	S
(18) West Selox	DM	Au	S
(19) Pat	Tv	Hg	un

[1] Approximately in decreasing order of significance; prospects named for claim names. Numbers refer to Figure 1

[2] Abbreviations as in Figure 1

[3] S = silicification and decalcification, Al = alunite, Ba = barite, argil. = argillic alteration with quartz veins, skarn = diopside ± actinolite ± marble, un = uncertain

leozoic miogeoclinal sediments deposited along the western edge of the North America craton are the predominant lithologies in the area. This stratigraphy consists of shelf facies marine carbonates with intercalated mudstones. The area lies approximately 40 km east of outcrops of rocks emplaced as part of the Roberts Mountain allochthon (Stewart, 1980). Evidence for Mesozoic-age igneous activity, metamorphism, or deformation is lacking in the immediate area, but it is prominent in nearby areas such as the Ruby Mountains (Barton, 1989). Post-Paleozoic rocks are predominantly Tertiary volcanic and lacustrine sedimentary rocks. Regionally, this part of the Great Basin is the site of highly variable amounts of Tertiary extension and magmatism, mainly in the Oligocene (Miller et al., 1988). However, the amount and nature of extension in the study area has not been investigated in detail.

District Geology

The district is composed predominantly of intercalated Paleozoic carbonates and shales (Hose and Blake, 1976). Dolostones are the principal lithology below the Upper Devonian; limestones and mudstones are the major rock types above. Mid-Cambrian through Mississippian rocks are exposed in the northern half of the district, whereas Devonian rocks are the oldest exposed strata in the southern half of the district. Upper Mississippian rocks consist of westerly derived, coarse clastic material that was shed from the Roberts Mountains allochthon. Regionally, the stratigraphic succession strikes north-south and dips east (Fig. 1). Many contacts between older units have been mapped as high-angle faults (Hose and Blake, 1976), but only in rare instances do these faults interrupt the normal stratigraphic succession. Tertiary volcanic and sedimentary rocks are restricted in exposures mainly to the southern portion of the district and to the Maverick Springs Range to the northwest. Tertiary rocks consist of andesitic flows and latitic lake sediments which generally lie disconformably on Mississippian strata. Quaternary alluvium, derived mainly from Paleozoic rocks, covers most low-lying areas.

The Bald Mountain stock and related dikes are the only intrusive rocks exposed in the district. The stock occupies much of the area between Big and Little Bald Mountains (Fig. 1). It is a composite body composed primarily of quartz monzonite with lesser amounts of granodiorite (IUGS classification, Blake, 1964). The body trends northwest and crops out over an area of 7 km^2. Quartz-feldspar porphyry dikes are quite abundant near the southeastern margin of the stock. The age of the stock is not known, but petrographically it resembles Tertiary granodiorite stocks in White Pine County (Hose and Blake, 1976). A small leucocratic dike similar to the dikes associated with the stock is present about midway between the Vantage deposits and Bald Mountain.

North- to northeast-trending high-angle normal faults define two horst blocks that are responsible for most of the topographic relief in the district. The western, Bald Mountain horst is formed by the southern extension of normal faults that uplifted the Ruby Mountains. The eastern, Alligator Ridge horst extends into the Maverick Springs Range that lies to the north-northeast (Fig. 1). These faults are, for the most part, obscured by Quaternary cover and appear to terminate at about the latitude of the southern end of Alligator Ridge. The area between the two horsts, known as Mooney basin, is a narrow graben filled with Quaternary sediments. The Vantage basin, which contains the Vantage deposits, is the southernmost extension of Mooney basin.

Gold mineralization and related alteration is widely distributed in the district (Fig. 1). Jasperoid bodies formed by quartz replacement of massive carbonate rocks are the most widespread form of hydrothermal alteration. These bodies are most common in the Upper Devonian Devils Gate Limestone at the contact with the Pilot Shale. Jasperoid is also present in the Mississippian Joana Limestone and the Ordovician Pogonip Limestone and to a lesser extent in dolostones. Gold mineralization associated with the Bald

Mountain stock was found in both the stock and nearby sedimentary rocks. A stockwork of quartz veins with argillic alteration of wall-rock feldspar was present in the stock (Hill, 1916). Relict sulfides consisted of chalcopyrite and pyrite, and copper and iron oxides were widespread. Carbonate rocks in contact with the intrusion were altered to garnet + wollastonite ± diopside skarn and marbles or were completely silicified. At the southeast end of the intrusion (Horseshoe prospect, Fig. 1), alteration was predominantly jasperoid replacement after Devils Gate Limestone. Sericitized igneous fragments present in the jasperoid indicate that the intrusion predates silicification.

Deposit Setting

Stratigraphy

The Vantage deposits were clustered in the northeastern portion of the Vantage Basin (Fig. 2). Mid-Devonian through Tertiary rocks are present in this small topographic basin. The oldest rocks exposed in the basin are medium gray, saccharoidal dolostones of the Nevada Formation. Regionally, the Nevada Formation is up to 900 m thick (Nolan et al., 1956), but only the upper 200 m are exposed in the Vantage Basin. Together with dolostones of the lower portion of the Devils Gate Limestone, the Nevada comprises Alligator Ridge. It appears to have been unaffected

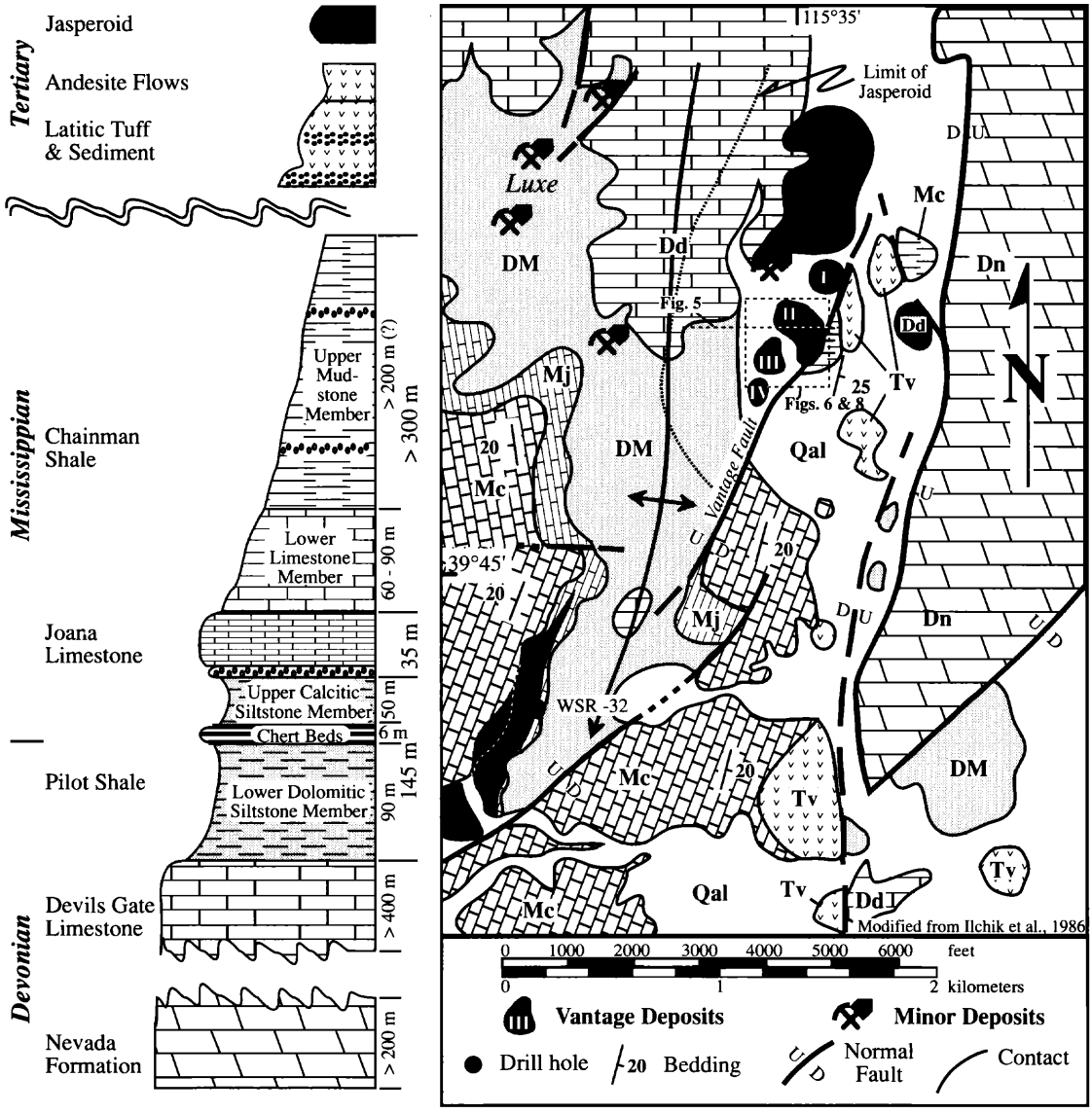

FIG. 2. Geologic map and stratigraphic column for the Vantage basin.

by hydrothermal activity in the vicinity of the Vantage deposits.

The Devonian Devils Gate Limestone overlies the Nevada Formation (Nolan et al., 1956). In the Vantage area, the Devils Gate consists of a lower dolostone sequence and an upper limestone sequence, but a complete section is not exposed. Approximately 250 m of dolostone are present on Alligator Ridge, and approximately 150 m of limestone are exposed to the northwest of the deposits (Fig. 2). The limestone is a 1- to 2-m bedded, ledge-forming micrite, with sparse fossil material, and formed the footwall of the Vantage deposits.

The Pilot Shale conformably overlies the Devils Gate Limestone. It is a thinly laminated (1–2 mm), 140-m thick sequence consisting mainly of distal turbidite deposits (Gutschick and Rodriguez, 1979). The formation is divided into lower and upper units in the Vantage Basin (Ilchik et al., 1986). The lower unit is the main host rock for the Vantage deposits. Where unaltered, it is a siltstone (average grain size ~ 40 μm) consisting of 30 to 40 percent illite (± minor kaolinite) and dolomite, 10 to 15 percent detrital quartz, 2 to 5 percent pyrite, 1 to 3 percent organic matter, and trace amounts of mica (Table 2 and Fig. 3A and B). Quartzose sandstones and chert beds, 1 to 10 cm thick, serve as local marker horizons in this unit. The upper unit is composed of calcite-bearing siltstone, which is similar to the lower unit except for the presence of calcite, and fossiliferous, silty limestone. It contains some hydrothermal calcite veins in the vicinity of the ore deposits but does not host any ore. A sequence of black chert beds, approximately 6 m thick, separates the two units.

Paleozoic strata overlying the Pilot Shale in the vicinity of the Vantage deposits include the Mississippian Joana Limestone and the Chainman Shale. The Joana Limestone is a bioclastic limestone composed mainly of crinoid debris and contains scattered bands of chert (Brew, 1971). A minor disconformity marked by a 3-m-thick orthoquartzite is present between the Pilot Shale and the Joana. The Joana is approximately 35 m thick. Overlying the Joana is the Chainman Shale. The lower portion of the Chainman is a fine-grained, thin-bedded limestone. The upper portion is a pyritic, carbonaceous mudstone. The Chainman is reported to be 300 to 400 m thick (Rigby, 1960) but is not well enough exposed in the area to measure. In the Vantage Basin, Tertiary rocks rest disconformably on the Chainman. Elsewhere in the area of Figure 1, the Diamond Peak Formation, coarse sandstones, and conglomerates with intercalated limestones overly the Chainman.

Cenozoic rocks in the area of the deposits consist of Tertiary volcanic rocks and related sediments and Quaternary gravels and alluvium. Lacustrine tuff-

TABLE 2. Mineralogy of Alteration Types

Alteration type	Primary[1]	Additions[2]	Removed[3]
	Pilot Shale protolith		
Unaltered[4]	Dol, il, q, py, OM	—	—
Calc. carb. siltstone (CCSl)[5]	Il, q, dol, py, OM	Cc, (cc ± orp ± real, kao)	Dol
Carbonaceous siltstone (CSl)	Q, il, py, OM	Q, asp, apy, (q + kao + sb)	Dol, cc
Alunite-bearing oxidized siltstone (OISl)	Q, trace il	Q, (alu ± ba, hm, goe[6])	Il, sulfides, OM
Maroon oxidized siltstone (MOSl)	Il, dol, q	Cc, hm	Dol, sulfides, OM
Oxidized w/minor carbon (OcSl)	Q, il, ±OM	Jar, SbOx	Sulfides, ±OM, il (?)
Calc. oxidized siltstone (CaSl)	Dol, il, q, trace OM	Cc, FeOx (?)	Sulfides, ±OM
	Devils Gate protolith		
Limestone	Cc, ba (?)	(Cc)	—
Jasperoid	Ba (?)	Q, sb, (cc, ba)	Cc

Mineralogy listed by decreasing abundance: alu = alunite, apy = arsenian pyrite, asp = arsenopyrite, ba = barite, cc = calcite, dol = dolomite, FeOx = undetermined brown iron stain, goe = goethite, hm = hematite, il = illite ± kaolinite, jar = jarosite, OM = organic matter, orp = orpiment, py = pyrite, q = quartz, real = realgar, sb = stibnite, SbOx = stibiconite; ( ) indicates vein mineral; see Figure 4 for paragenetic relationships between alteration types

[1] "Primary" refers to minerals present prior to hydrothermal activity and remaining to present day

[2] "Additions" refers to minerals introduced by alteration activity

[3] "Removed" refers to minerals destroyed or leached from rock; if mineral appears under both Primary and Removed, it indicates incomplete destruction

[4] Samples from WST-32 (Fig. 2); trace amounts of the following detrital minerals are also present: muscovite, mixed layer clay, zircon, plagioclase, and apatite

[5] Samples collected within 150 m of orebodies

[6] Goethite coats barite, thus it is later than most minerals in this stage and may have formed during a later (weathering?) event; jarosite veinlets are also present throughout much of this alteration type, but they crosscut both quartz-kaolinite-stibnite veins and alunite ± barite veins

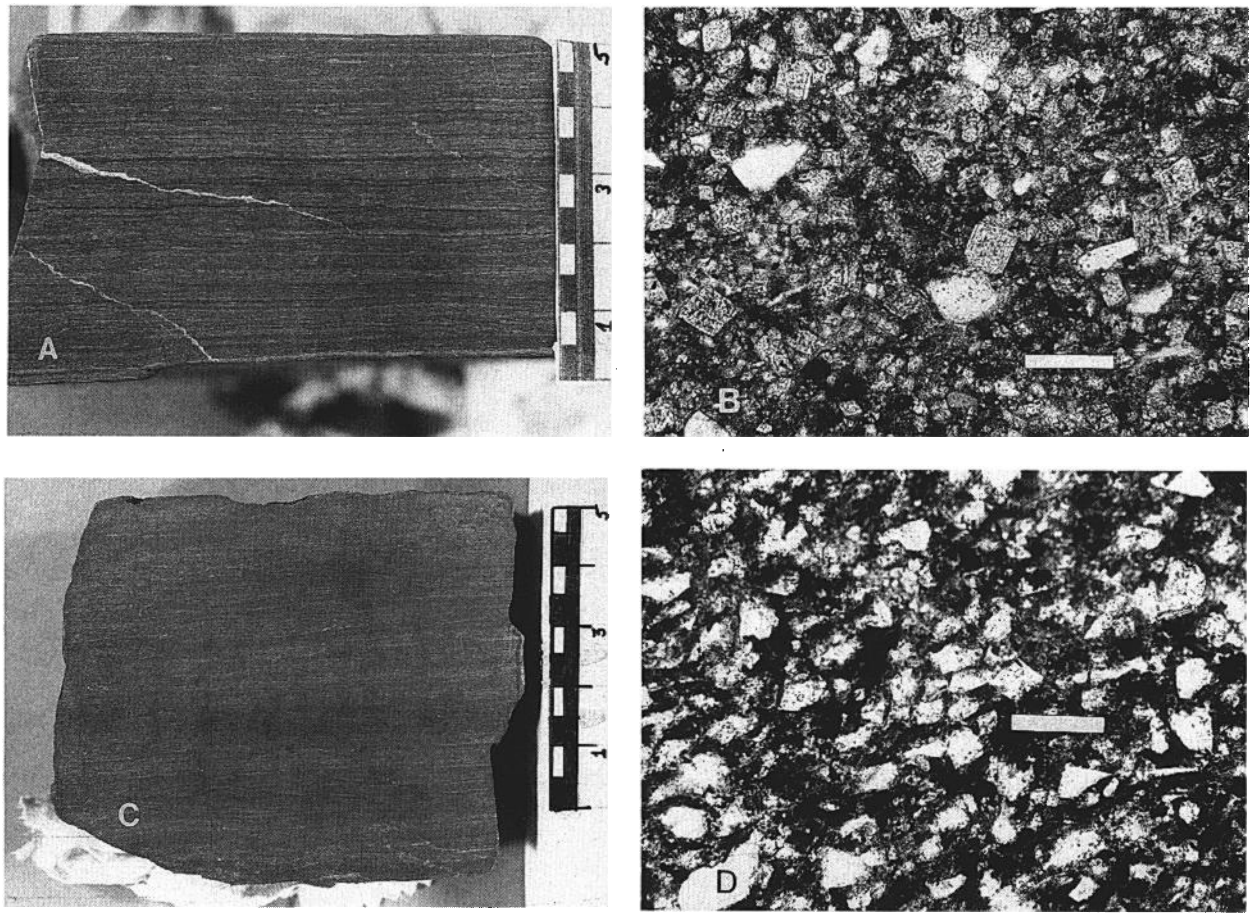

FIG. 3. Hand samples and photomicrographs of important alteration types. (Scale bar = 100 μm in photomicrographs, others in cm) A. Hand sample of calcareous carbonaceous siltstone with calcite veins, 6380 level, Vantage II. B. Photomicrograph of calcareous carbonaceous siltstone: rhombohedral grains are carbonate, clear grains are detrital quartz, opaques are pyrite, matrix is illite with organic matter. C. Hand sample of carbonaceous siltstone, 6380 level of Vantage II. Note that frequency of bedding laminations is similar to sample in A. D. Photomicrograph of carbonaceous siltstone showing rhombohedral shape of replacement quartz (clear). Matrix as in B. E. Photomicrograph of jasperoid composed of euhedral quartz with micron-sized inclusions of carbonate (crossed polars). F. Hand sample of alunite-bearing oxidized siltstone. Vein quartz fills early breccia space. Quartz is rebrecciated and cut by alunite (white). Jarosite veinlets (not visible) cut both quartz and alunite. G. Photomicrograph of alunite-bearing oxidized siltstone. Matrix is predominantly fine-grained quartz and was strongly altered by oxidation. Minor illite and coarser quartz from earlier events are also present. H. Photomicrograph of noncalcareous weathered siltstone. Matrix is similar to carbonaceous siltstone in D and was generally unaltered by weathering. Opaque is Fe oxide.

aceous sedimentary rocks up to 50 m thick are present east of the ore deposits (Fig. 2). These rocks are intermediate to felsic in composition and generally are altered to smectites. A red-brown weathering andesite flow overlies these lacustrine rocks in the vicinity of the ore deposits, but in the southern portion of the basin this rock rests nearly conformably on the Chainman Shale. Cooling features and brecciation of the andesite in this area indicate that this may have been a vent for the flow. Up to 20 m of Quaternary gravel covered previously exposed portions of the Vantage I and II orebodies and most of the premining surface in the vicinity of the deposits.

Structure

Two major normal faults are present in the Vantage basin. One is the fault along the west side of the Alligator Ridge horst. This fault consists of several strands distributed across a zone 50 to 100 m wide. Stratigraphic offset is estimated at between 600 and 1,000 m. Timing relations between this fault and hydrothermal activity are not known conclusively, but

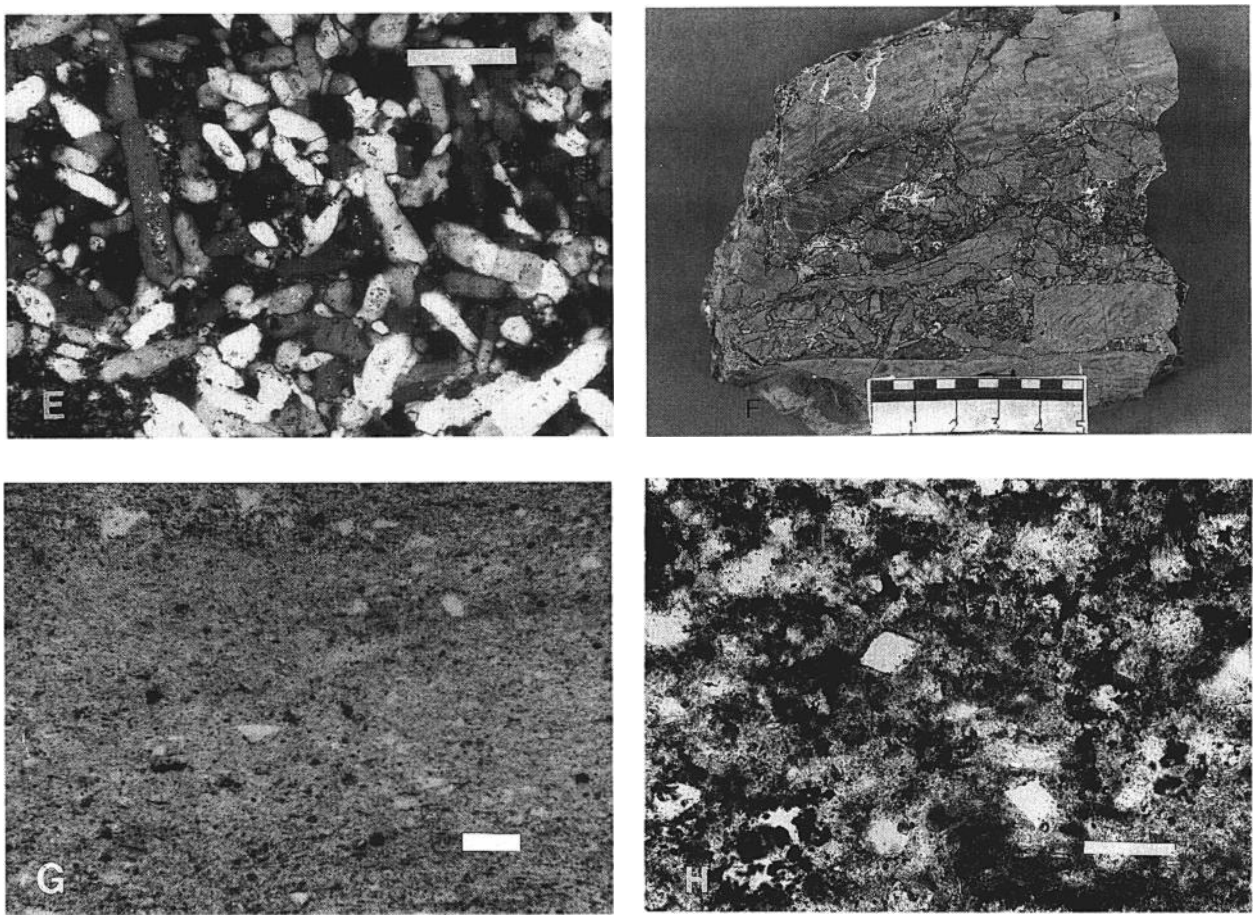

FIG. 3. (*Cont.*)

exposures of brecciated Devils Gate jasperoid in the fault zone suggest that the fault is postmineralization. The breccia consists of rounded, cobble-sized jasperoid fragments, with ~20 percent open space partially filled with late calcite. It is unlikely that Devils Gate limestone could retain this much open space during faulting; therefore, the jasperoid was probably formed prior to brecciation. A further indication that Alligator Ridge is a postmineralization feature is found at the Gator prospect (Fig. 1). Here, mineralization is truncated by normal faults of the horst.

The other major fault in the Vantage basin is a north-northeast-trending, east-dipping normal fault (Fig. 2). It is referred to as the Vantage fault because it is located just east of the orebodies. The fault is a zone approximately 30 m wide and divides the basin approximately in half. Displacement on the fault is estimated to be 200 to 300 m. The western footwall block exposes upper Devils Gate Limestone through basal Chainman Shale. Rocks in the footwall are folded into a north-northeast-trending anticline that roughly parallels the Vantage fault and plunges to the south. All known Au mineralization in the Vantage basin occurs within this block, and the four Vantage orebodies form an 800-m-long trend that parallels fault. The eastern, hanging-wall block consists of exposures of lower to upper Chainman Shale and Tertiary rocks.

The timing of movement on the Vantage fault relative to mineralization was inferred from geochemical evidence. Near the orebodies, organic matter in rocks on opposite sides of the fault was maturated by hydrothermal activity to similar levels that were well in excess of levels found elsewhere in the basin (Ilchik et al., 1986). Likewise, the As concentration in rocks adjacent to the orebodies was up to 500 ppm. This anomaly extended across the fault a short distance into the hanging wall (J. C. Ainsworth, pers. commun., 1983). These data indicate that the rocks on opposite sides of the fault were in juxtaposition at the time of hydrothermal activity.

Mine geology

The premining surface geology in the vicinity of the deposits was generally obscured by Quaternary

gravels. The only exposure of the orebodies prior to mining was a small outcrop of Vantage I. Several barren outcrops of Pilot Shale existed between Vantage I and II. East of the deposits were isolated exposures of Joana Limestone, Chainman Shale, and Tertiary rocks. Some of the exposures of Joana Limestone were silicified and encrusted with jarosite but contained <0.01 ppm Au. The only extensive premining exposures were those of Devils Gate jasperoids on a small hill north of the deposits (Fig. 2). These outcrops are part of the erosional-resistant basal alteration zone. Quartz veins with stibnite occur at several locations on this hill. Additional Au mineralization probably existed above these jasperoids but has been removed by erosion. Alteration elsewhere in the basin is restricted to silicification of the Joana Limestone and basal Chainman Shale in the southwestern portion of the basin. This jasperoid is barren of gold and overlies unaltered and unmineralized Pilot Shale.

A series of stair-step, northwest-trending, south-dipping normal faults, with displacements of about 30 m each, are present in the area of the deposits and extend to the Luxe area. These faults produced progressively shallower levels of exposure from the northern jasperoid to Vantage IV and appear to separate the major orebodies. Within each deposit overall stratigraphic continuity was generally maintained, although numerous minor normal and reverse faults were present. Breccias associated with these faults varied in intensity from local disruptions accompanied by drag folds to rubble zones up to 15 m wide. Offsets across these breccia zones, as determined by local marker beds, were commonly less than 5 m. Evidence for timing of these minor faults is equivocal, because replacement associated alteration was lithologically selective and followed specific lithologies regardless of structural position. The northwest-trending faults appear to be temporally related to the Vantage fault, and therefore should also be premineralization. Crushed fragments of quartz-kaolinite-stibnite or alunite ± barite veins in some breccias, however, are unequivocal evidence for minor syn- or postmineralization fault movement.

Crackle and mosaic breccias were widespread in the lowest 30 m of the Pilot Shale within the deposits. The breccias were formed by the intersection of closely spaced fractures (5–20 cm) and bed partings. The intensity of brecciation increased as the jasperoid contact was approached. Only minor movement of the clasts was present in the upper portion of the breccia, giving the rock a crackled appearance. Near the jasperoid contact, some clasts were rotated, and the breccias had a mosaic texture. Fractures in these breccias were generally coated with jarosite. Chert beds in the siltstone could be traced for considerable distance through these areas and showed that vertical displacements associated with brecciation were negligible. The style of brecciation suggested a settling process, possibly related to the caverns underlying the area, and the presence of jarosite (see below) indicates that these breccias formed late in the history of the deposits.

Several large caverns are present beneath the deposits, at or just below the jasperoid-limestone contact. These caverns are areas of several thousand square meters and are up to 10 m high. They are probably a recently developed karst due to channeling of subsurface waters along this contact, and they may be partially responsible for the collapse breccias described above.

Geochronology

Geologic constraints indicate that mineralization postdates movement on the Vantage fault and predates uplift of Alligator Ridge. Tertiary volcanic and sedimentary rocks are displaced along the Vantage fault and thus also predate mineralization. Data for Tertiary volcanic rocks in this part of the Great Basin indicate a range in ages from 39 to 24 Ma (Gans et al., 1989). The age of high-angle faulting associated with the uplift of Alligator Ridge is poorly constrained but postdates volcanism.

Radiometric dating of materials from the Vantage deposits is limited to K-Ar data on alunite associated with postgold deposition oxidation. Radiometric dating of the ore-forming event is not possible, because minerals associated with decalcification and Au deposition are not suitable for these techniques. K-Ar dating on alunite has given dates which are concordant with other constraints at several epithermal deposits (e.g., Ashley and Silberman, 1976; Cunningham et al., 1984), but little is known about its Ar retention properties. Likewise, the relations between gold deposition and oxidation in the Vantage deposits remain debatable (see below). Thus, interpretation of the alunite dates relative to gold deposition is speculative.

Seven alunite samples from a variety of environments were dated by standard K-Ar methods (Table 3). Dates from four of the samples are tightly clustered at 11.5 ± 0.7 Ma. Dates for the other three samples vary from 9.1 to 3.6 Ma. SEM energy dispersive analyses indicate that alunite was intergrown with submicroscopic quartz and an aluminosilicate (kaolinite?), and macroscopic barite was visible in the samples from fully oxidized rocks. Grain size varied from 0.5 to 4 μm and grain shapes varied from platy (sample VD-7-449) to equidimensional (sample II-38.8-1). The intergrowths account for the low K_2O content of the samples, but no systematic relations between grain size, shape, or K_2O content and age were found.

Interpretation of the alunite data is complicated by the uncertainty of its origin. One interpretation, based on a supergene origin, is that alunite formed over the entire time span indicated. In this case, the duration

TABLE 3. K/Ar Dates on Alunite

Sample no.	Apparent age (Ma)	% K_2O	Location	Host rock[1]
II-38.8-1[2]	12.4 ± 0.5	7.60	VII, 6380 level	OISl, overgrown by late calcite
II-38-2A[3]	11.3 ± 0.2	8.21	VII, 6380 level	OISl, overgrowth on barite
II-38.24-5[3]	11.2 ± 0.2	9.22	VII, 6380 level	CSl at OISl contact
VD 22-295[2]	10.9 ± 0.5	3.45	VII, 6314 elev	Jasperoid-limestone contact
II-38.8-3[2]	9.1 ± 0.4	8.65	VII, 6380 level	OISl, with calcite and rock fragments
- - -[3]	8.3 ± 0.3	na	VI	Jasperoid, intergrown with barite
VD 7-449[2]	3.6 ± 0.2	8.16	VII, 6190 elev	Jasperoid-limestone contact

[1] Abbreviations as in Table 2, na = not available

[2] Personal communication, 1986, Geochron Laboratories, Cambridge, MA 02139; radiometric constants: $\lambda_\beta = 4.962 \times 10^{-10}$/yr, $(\lambda_e + \lambda_{e'}) = 0.581 \times 10^{-10}$/yr, $^{40}K/K = 1.193 \times 10^{-4}$ g/g

[3] Personal communication, 1986 and 1987, W. Bagby, USGS, Menlo Park, CA 94025; radiometric constants: $\lambda_\beta = 4.963 \times 10^{-10}$/yr, $(\lambda_e + \lambda_{e'}) = 0.581 \times 10^{-10}$/yr, $^{40}K/K = 1.167 \times 10^{-4}$ g/g

of weathering would actually be much greater than suggested, because these dates would be growth integrated, or average, ages. If a constant growth rate is assumed, then nucleation of the samples would have occurred at approximately twice their indicated age. Thus, weathering would have begun very shortly after the cessation of volcanism in the area and close to the upper constraint in age. In a supergene scenario, the dates also should be randomly distributed due to variations in time of nucleation, and dates from a single sample could be variable. However, the dates are clustered near 11 Ma and the reproducibility of ages was ±0.3 Ma for duplicate analyses. An alternative interpretation based on a hypogene origin is that Ar loss occurred, and thus, some or all of the dates are misleadingly young. This interpretation is supported by crosscutting relationships with minerals formed during weathering (e.g., jarosite and late calcite) and is the interpretation preferred here based on reasons presented below. However, regardless of the mode of origin, the 11.5 ± 0.7 Ma date represents a minimum age for the mineralization.

Alteration

Introduction

Alteration and metal distribution in the Vantage gold deposits appear to be the result of a sequence of three events. The first of these involved the replacement of carbonates in the Pilot Shale and Devils Gate with quartz. Precious metals, As, and Sb were deposited in carbonaceous siltstone and jasperoid at this time. Subsequently, an early oxidation event destroyed pyrite, organic matter, and illite in the Pilot Shale and produced alunite ± barite veins. Metals introduced during the replacement event were redistributed, but no additional metal was introduced. The origin of this oxidation is equivocal, but it is thought to be related to the late stages of hydrothermal activity. Finally, processes associated with weathering produced a second oxidation event that also destroyed pyrite and organic matter and produced jarosite veinlets, but it had little effect on the matrix of the siltstone or metal distribution. Paragenetic relations for the various alteration types produced by these events and their protoliths are shown in Figure 4.

Decalcification and silicification

The replacement of carbonate minerals in both the Pilot Shale and Devils Gate Limestone with quartz was the alteration most consistently associated with ore in the Vantage deposits. Crosscutting features and the spatial distribution of silicification indicated that this was the earliest alteration event in the formation of the deposits, whereas metal distribution indicated that this was the only event that introduced significant amounts of precious metals.

Replacement of carbonate with quartz altered the Pilot Shale to a noncalcareous, carbonaceous siltstone, referred to as carbonaceous siltstone (Fig. 3C and D). The mode of quartz increased from about 15 percent to 30 to 40 percent. Silicification, however, did not alter the fabric of the siltstone appreciably and the rock remained soft and poorly indurated (e.g., compare Fig. 3A with Fig. 3C). Replacement quartz generally occurred as pseudomorphs of dolomite rhombohedra (Fig. 3D) and in rare cases, partially replaced carbonate was intergrown with quartz. These observations indicate that volume was approximately conserved during replacement.

Sulfides present in the carbonaceous siltstone included stoichiometric pyrite, arsenian pyrite, arsenopyrite, and stibnite. Stoichiometric pyrite occurred as cubes or framboids less than 40 μm in size and was intergrown with organic matter. This pyrite was probably diagenetic. Arsenian pyrite contained 1.0 to 1.5 wt percent As (electron microprobe analyses) and was present as overgrowths on stoichiometric pyrite and as disseminated grains. Similar arsenian pyrite

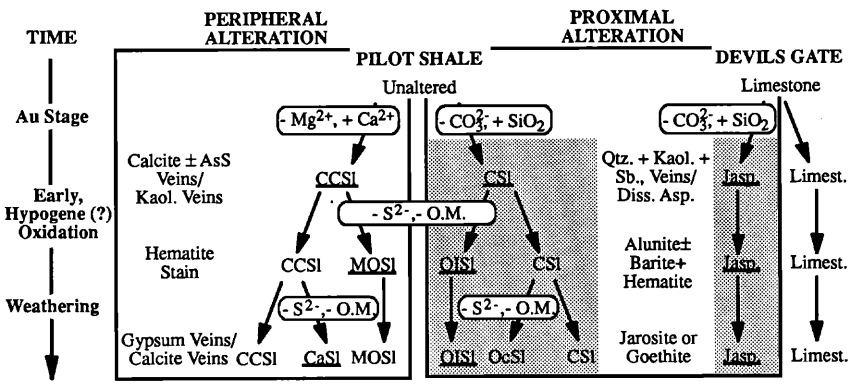

FIG. 4. Schematic diagram of time and space relationships between alteration types. Time progresses downward and, for the Pilot Shale, distance from deposit centers increases to the left. Au-bearing rocks are highlighted and vein assemblages are in underlined rock types. See Table 2 for alteration-type abbreviations. Major compositional gains (+) and losses (−) are shown in boxes between alteration types. SiO_2 = aqueous silica, Mg^{+2} = magnesium, Ca^{+2} = calcium, CO_3^{-2} = dolomite and/or calcite, S^{-2} = sulfides, and O.M. = organic matter.

was present in other Carlin-type deposits (Wells and Mullens, 1973). Arsenopyrite (~45.5 wt % As, electron microprobe analyses) occurred as distinct grains less than 80 μm in diameter and was disseminated in the siltstone. Stibnite generally occurred in veins with quartz (see below) or, in rare cases, as disseminated grains. Gold was not detected by microprobe examination of sulfides, nor were any Au-Ag minerals, cinnabar, or native arsenic found in carbonaceous ore.

Peripheral to silicification, indigenous dolomite in the Pilot Shale was replaced with calcite for at least 250 m beyond the orebodies. Dolomite was the only carbonate present in unaltered lower Pilot Shale. Calcite, however, was present in all samples along the cross section in Figure 5 and was the predominant carbonate at the decalcification fronts. The total carbonate content, as indicated by XRF data (see below), remained nearly constant at ~35 wt percent during this alteration. Carbonate content of the siltstone decreased only within several meters of the contact with noncalcareous rocks. Overall, carbonates were the only portion of the Pilot Shale grossly affected during this stage of alteration. The siliciclastic fraction of the siltstone appeared unaltered, and pyrite and organic matter, although matured, were retained (Table 2).

Hydrothermal activity matured organic matter in silicified and, to a lesser extent, in dedolomitized, carbonaceous siltstone. Maturation was shown by a decrease both in the H/C_{atomic} ratio of kerogen in the siltstone (Ilchik et al., 1986) and in the abundance of volatile hydrocarbons (R. M. Kettler, pers. commun., 1987). Pyrobitumen, an asphaltic, insoluble organic material, was found as a fracture filling in a few locations in the Vantage II deposit (Ilchik et al., 1986). Similar material was present in the Carlin deposit (Hausen and Kerr, 1968). Quartz-kaolinite veins crosscut the pyrobitumens, indicating that the pyrobitumens were introduced prior to the vein minerals. Ilchik et al. (1986) suggested that pyrobitumens were residual products of maturation of Pilot Shale kerogen. Based on an inferred thermal history of the region which modeled burial heating, they concluded that this material was Mesozoic in age and therefore was introduced prior to the formation of the Au deposits.

Replacement of carbonate by quartz in the Devils Gate Limestone was similar to that in the Pilot Shale and produced a jasperoid composed of >95 modal percent quartz (Table 2). The quartz formed mattes of interlocking, euhedral crystals 10 to 200 μm in size (Fig. 3E) which generally contained 1 to 3-μm-size inclusions of relict calcite. Barite was the only other mineral commonly present in jasperoid. It occurred as dispersed euhedral crystals, aggregates of crystals, or concordant bands that appeared to be of a sedimentary origin. In hand sample and outcrop, the jasperoid was massive and thus texturally similar to the limestone protolith. Locally, however, fossils and sedimentary textures were preserved in the jasperoid.

Two sets of veins were associated with this alteration. Quartz-kaolinite-stibnite veins were present in the central portions of the orebodies. The veins were <1 mm to ~1.5 cm wide and typically contained subequal portions of quartz and kaolinite (or dickite) and 5 to 10 vol percent stibnite. Areas with >6 ppm Au typically had several veins per meter, but visible gold was not found in these veins in unoxidized ore. Monomineralic kaolinite veinlets, rarely exceeding 1 mm in width, were ubiquitous in noncalcareous siltstone outside of the high-grade areas and were present in calcareous siltstone up to 75 m from ore. These kaolinite veins are viewed as lateral equivalents of the quartz-kaolinite-stibnite veins. The second set of veins were calcite-bearing veins found primarily in calcareous siltstone and limestone adjacent to decal-

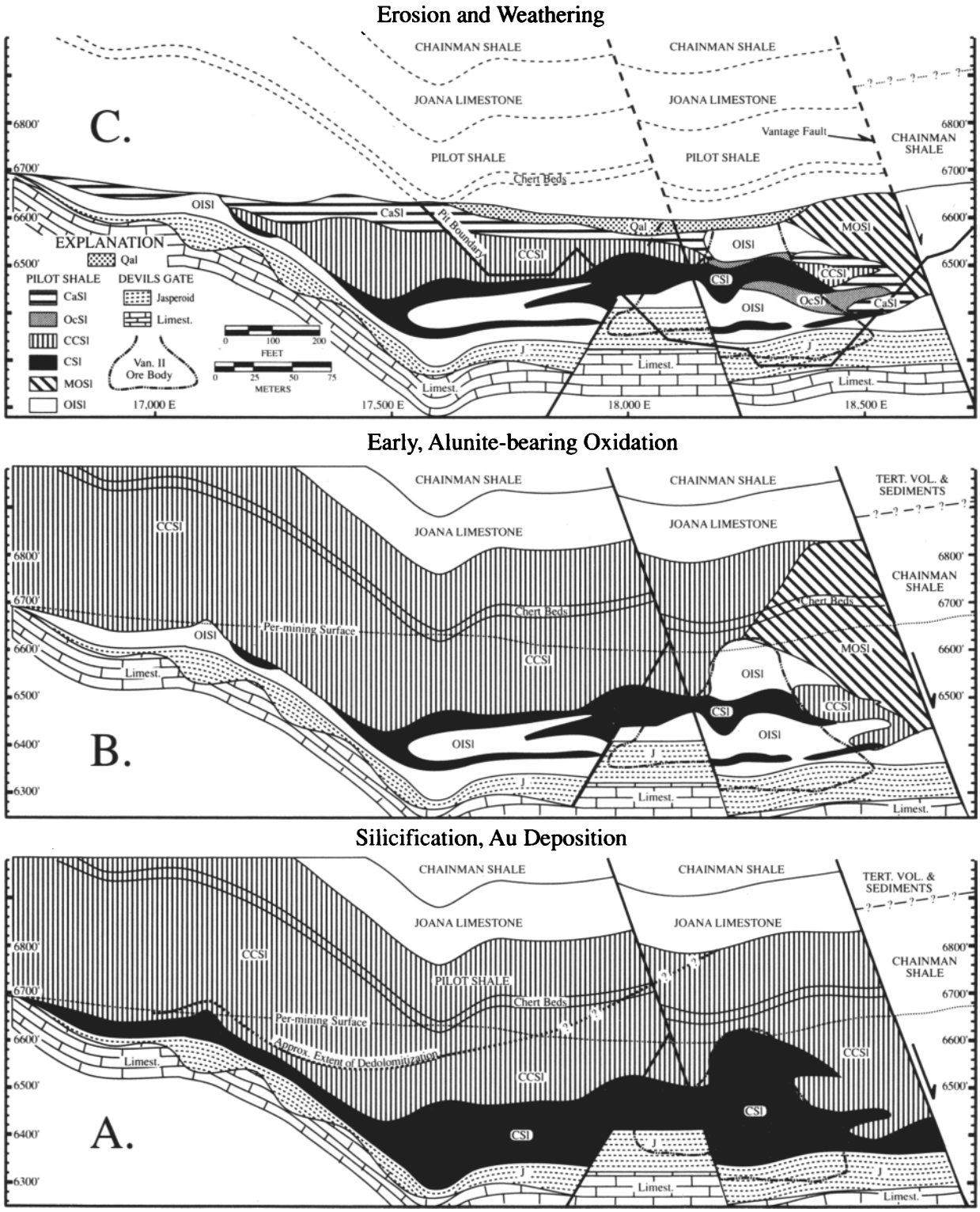

FIG. 5. Cross section through Vantage II orebody and adjacent areas showing the major stages in the temporal development of relationships between alteration types and stratigraphy. Data from pit mapping and surface drilling (see Fig. 8 for locations of most drill holes, others at 100-ft intervals). See Table 2 for alteration type abbreviations. A. Primary alteration associated with Au deposition. B. Early alunite-producing oxidation event. C. Premining configuration. Note that the alluvial surface cuts the orebody, indicating that significant erosion occurred subsequent to mineralization. Stratigraphy above premining surface was constructed from local measurements and probably represents the minimum cover at the time of ore deposition.

cified areas. The veins were between 0.1 to 20 cm in width. They appeared abruptly at the contact between noncalcareous and calcareous rocks and extended at least 150 m beyond this contact. Calcite veins were generally monomineralic, but within 20 m of the orebodies they often contained up to 50 vol percent orpiment ± realgar. The abundance of calcite veins was several per meter at the contact with decalcified rocks and decreased outward (Fig. 6A and B). The spatial extent beyond the limits of mining was hard to determine due to the lack of exposures.

Oxidation

Oxidation following precious metal deposition dramatically altered the Pilot Shale by destroying organic matter and sulfides throughout much of the deposits. The Devils Gate lithologies, however, appeared unaffected by oxidation except for the introduction of sulfate-bearing veins because they generally lacked reduced species. Oxidation in the deposits was subdivided into two types based upon differences in mineralogy, texture, distribution, crosscutting relations, and timing. The early type of oxidation was distinguished by the complete destruction of sulfides and organic matter, the presence of alunite and/or barite veins, and the destruction of phyllosilicates in the siltstone that resulted in substantial textural modifications of the siltstone matrix. Its distribution was similar to but more restricted than the distribution of the silicification (Fig. 6A and B) and suggested a hydrothermal origin. The second type of oxidation was characterized by the presence of jarosite or goethite, incomplete destruction of organic matter, and a lack of appreciable textural modifications to the siltstone. Spatially, its distribution was related to the premining erosion surface or fractures that extend from the surface, and thus appears related to weathering.

Early, alunite-barite oxidation: Complete removal of organic matter and sulfides, formation of alunite ± barite veins, and induration of the siltstone matrix characterized this type of oxidation. The destruction of organic matter left the siltstone pale gray in color, which generally was modified to maroon by minute

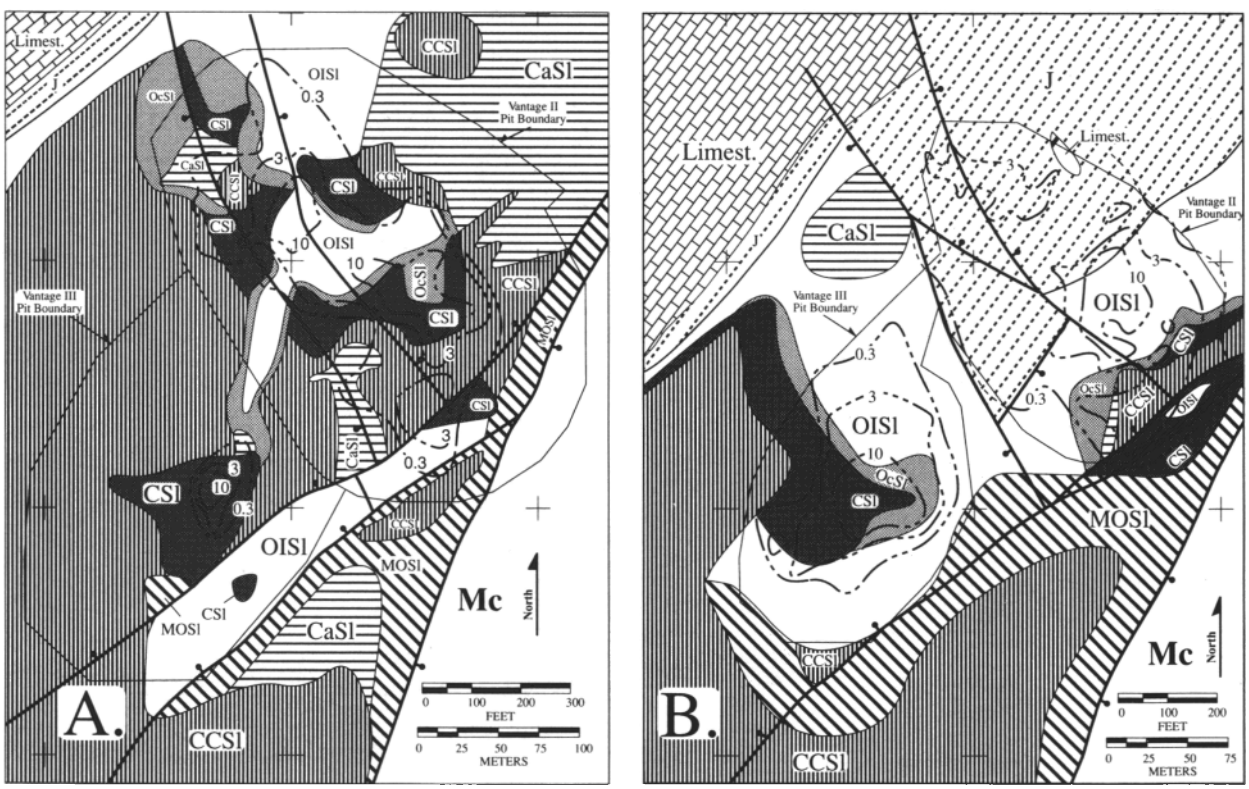

FIG. 6. Level maps of the Vantage II and III deposits with Au grade contours (in ppm). Symbols as in Figure 5. A. 6480 level showing contact relations between Pilot Shale alteration types. Vantage II area shows relations in upper portion of orebody; Vantage III area shows relations immediately above orebody. B. 6380 level showing stratiform contact between Pilot Shale and jasperoid in Vantage II and mid-level of Vantage III orebody. Note the alignment between grades and ore thickness shown in Figure 8. Geologic data for Vantage II from pit mapping and drilling; for Vantage III mainly from surface drilling. Grade contours from 20-ft blast holes drilled on 4 × 4 m grid.

specks of hematite (Fig. 3F). The fact that this rock previously contained sulfides was indicated by the presence of bladed (stibnite) and cubic (pyrite) molds, but these sulfides were completely leached. The mode of illite decreased significantly in comparison to carbonaceous siltstone, and the mode of quartz increased to 80 percent or more (compare Fig. 3G with Fig. 3D). Trace amounts of mica remained after oxidation. The loss of bedding laminations accompanied destruction of illite, and the fabric of this rock was dominated by finely intergrown quartz. Klessig (1984) referred to this ore type as "silicified siltstone" because it was substantially harder than carbonaceous siltstone. This terminology is misleading, however, because silica was introduced during the earlier replacement period of alteration, whereas during oxidation the additional quartz was probably residual silica from the destruction of illite (see below).

Calcareous, unsilicified siltstone in contact with early, alunite-bearing oxidation on the eastern side of the deposits also was oxidized (Figs. 5 and 6A and B). Organic matter and sulfides in this siltstone were completely oxidized. The rock was either bleached white or stained maroon or orange by fine-grained hematite. The carbonate content was diminished to generally less than 15 percent. This type of alteration is referred to as maroon-oxidized siltstone. Kaolinite and calcite veins from earlier alteration were common, but no other veins were present. This alteration appeared to be the lateral equivalent of the early, alunite-bearing oxidized siltstone in calcareous siltstone which was not silicified during the earlier hydrothermal activity.

Veins of alunite and/or barite and fracture coatings of black hematite were widely distributed throughout the zones of oxidized and indurated siltstone and, to a lesser extent, in the jasperoid. Alunite ± barite veins crosscut quartz-kaolinite veins which contained bladed molds of stibnite. Tabular barite crystals associated with oxidation, 0.1 to ~1 cm in size, occurred distinctly as open-space fillings and were readily distinguished from the disseminated and bedded habits in jasperoid described above. Vein barite was usually overgrown by fine-grained alunite, but alunite was more widespread than barite. It generally occurred as monomineralic veins up to ~1 cm wide and was present throughout oxidized and indurated ore zones and in adjacent areas of carbonaceous ore. Alunite in oxidized ore was euhedral and from 15 to 150 μm in size. In rare instances, alunite showed oscillatory zoning with jarosite. Alunite ± barite veins in carbonaceous ore were present in a 2- to 3-m-wide transition zone adjacent to oxidized areas. Pyrite was partially to completely destroyed in these transition zones, and alunite had a reticular morphology and was finer grained (15–20 μm). This suggests that some recrystallization took place as oxidation progressed.

Weathering: This oxidation was spatially related to the premining surface and was superimposed on the products of both earlier alteration events. For these reasons it was assumed that it was produced by recent weathering and not the result of hydrothermal activity. Weathering resulted in the pervasive destruction of sulfides but only the partial removal of organic matter in rocks not previously oxidized. The effects of weathering were similar in both calcareous and noncalcareous siltstone. Both rock types were characteristically yellow-brown in color, presumably due to the presence of minute amounts of jarosite or goethite, and contained approximately 0.25 modal percent remnant organic matter (visual estimate). Stibiconite and jarosite, the oxidation products of stibnite and pyrite, respectively, were often present in the old sulfide sites rather than being completely leached as in the alunite-bearing oxidation. Also in contrast with the alunite-bearing oxidation, illite and the laminated texture of the siltstone were retained, and induration did not accompany weathering.

Veins formed during weathering were widely distributed in the Vantage deposits. Jarosite veinlets were the most common veins in the deposits. It occurred as encrustations of euhedral crystals, rarely exceeding 0.5 mm in size, on nearly all fractures in previously oxidized, alunite-bearing rocks. These fractures only rarely contain other vein minerals, but the fractures crosscut both quartz-kaolinite (with stibnite molds) and alunite ± barite veins. In noncalcareous carbonaceous ore, jarosite was present as pseudomorphs of pyrite and, to a lesser extent, on fractures. Goethite was present in the deeper portions of Vantage II near the siltstone-jasperoid contact. It coated barite crystals and broken fragments of quartz-kaolinite-stibnite veins. Goethite thus appeared to be contemporaneous with jarosite but was found in areas that were relatively removed from pyritic rocks. Late calcite was also present as fracture fillings in alunite-bearing oxidized siltstone and jasperoid. Late calcite covers alunite and barite and had spelean habits such as travertine and "cave popcorn." Gypsum veins were rare in weathered, calcareous siltstone, but kaolinite and calcite veins, inherited from earlier alteration, were present.

Major Element Chemistry of Alteration Types

Major element concentrations were determined on a suite of whole-rock samples from Vantage II and vicinity to assess mass transfer effects associated with alteration. Analyses were performed using standard XRF techniques on pressed powder pellets. Five oxides, K_2O, MgO, CaO, Al_2O_3, and SiO_2, plus S accounted for nearly all the major components determined by XRF. Na_2O was below detection (<0.1 wt %) in all samples and TiO_2 was generally less than 0.4 wt percent. Concentrations of carbonate and H_2O

were calculated from the XRF major element data, because these components could not be determined directly. Carbonate content was assumed to be 0.92 × CaO + MgO (MgO was corrected for illite composition, see below). H_2O was assumed to be 9 percent of illite, the only hydrous phase of major abundance. Illite norms for each sample were calculated from the concentration of Al_2O_3. Weight percents for the major oxides plus sulfur were then normalized to totals that included carbonate and H_2O.

Density measurements were made on hand samples of the various alteration types of the Pilot Shale and for jasperoid to determine volume normalization factors for comparisons of whole-rock data (Table 4). Unfortunately, drill cuttings were the only samples of unaltered Pilot Shale available and they were not suitable for density measurements. Density differences between all alteration types, except for weathered noncalcareous siltstone, were 4 percent or less, and all were within one standard deviation. Because of the similarities in densities of the alteration types, the whole-rock data are presented on a g/100g rather than on a g/cm^3 basis.

The major element data for the Pilot Shale were modeled as a system consisting of dolomite, calcite, illite, kaolinite, quartz, pyrite, and organic matter. The composition of illite, the only mineral potentially with large chemical variation, was estimated from the regression of K_2O vs. Al_2O_3 and SiO_2 vs. Al_2O_3 data for unaltered samples (Fig. 7B and D), and from MgO vs. Al_2O_3 data for carbonate-free samples. The estimated compositions were remarkably uniform at 63 wt percent SiO_2, 18 wt percent Al_2O_3, 2 wt percent MgO, 5.4 wt percent K_2O, and 9 wt percent H_2O, and are a typical illite composition (Woods and Garrels, 1987).

Eight fresh, unaltered samples of Pilot Shale had a normative mineralogy of 30 to 45 wt percent dolomite + calcite, 35 to 50 wt percent illite, 14 wt percent detrital quartz, 5 wt percent pyrite, 1.5 wt percent organic matter (Ilchik et al., 1986) and 0 to 3 wt percent kaolinite. These samples contained 15 to 30 wt percent CaO + MgO. Normative calcite to dolomite ratios were near zero for nine samples from the lower portion of the Pilot Shale and between 0.25 and 1 for four samples from the upper portion (Fig. 7A). In the lower portion, the MgO content relative to CaO exceeded that needed to form dolomite by 1 to 2 wt percent. This excess is consistent with the composition of illite given above. K_2O vs. Al_2O_3 and SiO_2 vs. Al_2O_3 data formed linear arrays that partly determined the composition of illite and represent mixing lines between dolomite and illite (sedimentary trends in Fig. 7B and D). This covariation of dolomite and illite is interpreted as sedimentologic. The normative quartz content of the samples is given by the SiO_2 intercept of the sedimentary trend (Fig. 7B), and the normative kaolinite content is proportional to the residual Al_2O_3 at zero K_2O (Fig. 7D). Iron in unaltered, carbonaceous samples varied between 1 and 3 wt percent and balanced with S near the composition of pyrite. Sulfur was depleted in weathered samples but FeO was unchanged.

Norms for ten calcareous carbonaceous siltstone samples from near the deposits were 10 to 45 wt percent calcite, 0 to 15 wt percent dolomite, 30 to 60 wt percent illite, 0 to 10 wt percent kaolinite, 20 wt percent quartz, and similar amounts of pyrite and organic matter to that found in unaltered samples. Sedimentologic substitution between dolomite and illite again accounted for much of this variation, but some hydrothermal effects were also present. Samples from the vicinity of the deposits had 7 to 28 wt percent CaO + MgO and normative calcite to dolomite ratios generally greater than unity (Fig. 7A). Normative ratios are minimum values, however, because of MgO present in illite. Ratios calculated assuming that 1 wt percent MgO was present as illite were higher and indicate that calcite is the only carbonate in approximately half of these samples. Density differences between calcite and dolomite explain the higher than background total CaO + MgO content in several of these samples relative to the average unaltered value. A slight excess of silica was present in some samples when compared with the sedimentary trends (Fig. 7B and C) and possibly indicates incipient carbonate removal and silicification. Alteration of illite to kaolinite and removal of K_2O is indicated by the low K_2O/Al_2O_3 ratio of some samples (Fig. 7D).

Norms calculated for 17 carbonaceous siltstone samples were 30 to 65 wt percent illite, 5 to 10 wt percent kaolinite, and 25 to 60 wt percent quartz. Calcite was less than 5 wt percent present in any sample. Pyrite and organic matter contents were similar

TABLE 4. Densities of Selected Alteration Types[1]

CCSl	CSl	OISl	OcSl	Jasperoid
2.46 ± 0.12 n = 15	2.37 ± 0.15 n = 20	2.43 ± 0.08 n = 15	2.12 ± 0.27 n = 13	2.36 ± 0.12 n = 8

[1] g/cm^3 with 1 σ; abbreviations as in Table 2

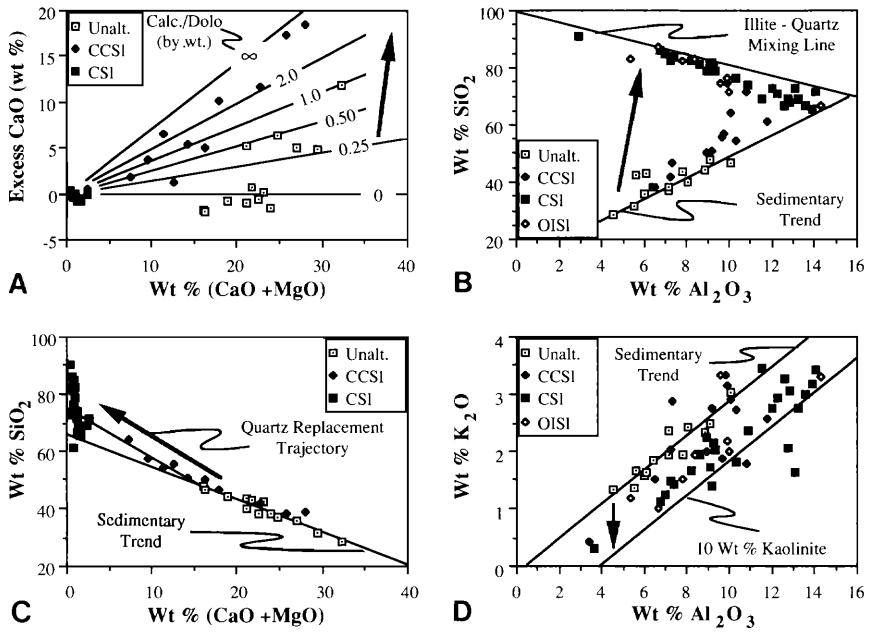

FIG. 7. XRF whole-rock major element data for Pilot Shale alteration types. Abbreviations as in Table 2. Sedimentary trends are regressions of data from unaltered samples (WSR - 32, Fig. 2). Calcareous carbonaceous siltstone (CCSl) samples are from the vicinity of the deposits. Gray arrows are vectors for constant volume replacement. A. (CaO + MgO) vs. CaO in excess of that required to form dolomite (0.72 × wt % CaO − wt % MgO) for unaltered, calcareous carbonaceous siltstone and carbonaceous siltstone (CSl). Values below zero for excess CaO in unaltered and carbonaceous siltstone samples indicate MgO content of illite. Unaltered samples with calcite to dolomite ratios of 0.25 to 1 were from the upper portion of the Pilot Shale which is not present in the area of the deposits. The high calcite content of calcareous carbonaceous siltstone samples are the result of dedolomitization. B. Al_2O_3 vs. SiO_2 for unaltered, calcareous carbonaceous siltstone, carbonaceous siltstone, and alunite-bearing oxidized siltstone (OISl). Sedimentary trend is consistent with substitution between dolomite and illite and a constant 14 wt percent detrital quartz (see text). Illite-quartz mixing line is the compositional limit imposed by illite on the amount of SiO_2 that can be present after decalcification. Removal of carbonate without silica addition would proceed along the sedimentary trend; volume conservative replacement of carbonate by silica would proceed along a nearly vertical path (gray arrow). Approximately half of the decalcified samples are incompletely silicified and probably have suffered some compaction. C. (CaO + MgO) vs. SiO_2 for unaltered, calcareous carbonaceous siltstone and carbonaceous siltstone. D. Al_2O_3 vs. K_2O for unaltered, calcareous carbonaceous siltstone, carbonaceous siltstone, and alunite-bearing oxidized siltstone (OISl) samples. Sedimentary trend indicates that only trace amounts of kaolinite were present in unaltered samples (proportional to residual Al_2O_3 at zero K_2O). Most altered samples showed some depletion in K_2O (or increase in Al_2O_3) indicating that up to ~10 wt percent kaolinite was present in these samples.

to unaltered samples. The complete removal of carbonate from these samples is shown by the low CaO + MgO content (Fig. 7C). The small amount of MgO present correlated with Al_2O_3 (not shown) and thus was probably present in illite. Simple leaching of carbonate during alteration would change compositions along the sedimentary dolomite-illite mixing trend of constant SiO_2/Al_2O_3 (Fig. 7B). SiO_2 vs. Al_2O_3 data, however, plotted close to a mixing line for illite and quartz. The slightly lower SiO_2 values were due to the presence of pyrite and other minor phases. Complete replacement of carbonate with silica would change compositions along a nearly vertical (slightly positive slope due to density differences) trajectory from unaltered compositions to the illite-quartz mixing line and would produce samples with 76 to 82 wt percent SiO_2. Incomplete silicification would produce compositions with lower silica that plot between the two mixing lines. About half of the samples plot in the area of complete, volume conservative replacement; the remaining samples probably had unsilicified void space and/or underwent some compaction after calcite removal. Alteration of illite to kaolinite, indicated by decreasing K_2O/Al_2O_3 (Fig. 7D), appears to have accompanied silicification.

Few whole-rock data are available for the oxidized alteration types, so no comparison can be made for these alteration types. Available data for alunite-

bearing oxidized samples showed only minor differences from that for carbonaceous siltstone in SiO_2, Al_2O_3, K_2O (Fig. 7B and D), and FeO. Presumably these elements were conserved during oxidation. Sulfur and organic carbon were depleted, however.

Alteration Distribution and Contact Relations

The area of known alteration was confined to the footwall of the Vantage fault and was crudely semicircular in plan with a radius of ~1 km (Fig. 2). Silicification was centered on and nearly coincident with the areas of Au mineralization. Silicification was in turn surrounded by an area of dedolomitization and calcite replacement. Decalcification and silicification were discordant to bedding in the central portions of the orebodies. Silicification was up to 60 m thick in the siltstone and 30 m thick in the Devils Gate Limestone. Silicification narrowed beyond the orebodies, and 150 m west of the deposits it was a nearly stratiform zone approximately 30 m thick along the Devils Gate Limestone-Pilot Shale contact (Fig. 5). Silicification south of the deposits was also confined along the sedimentary contact and pinched out along the Vantage fault 500 m south of Vantage IV. The extent of silicification is not known to the north, because only a thin veneer of subore-grade (0.05–0.5 ppm Au) jasperoid remains over unaltered limestone. Silicification was terminated to the east of the deposits by the Vantage fault and was not found in the Chainman Shale mudstones.

Early oxidation had a distribution that was similar to but more restricted than silicification. Alunite-bearing oxidation was generally confined to the deeper portions of the orebodies between the jasperoid horizon and an overlying carbonaceous blanket (Fig. 5). In the centers of Vantage I and II, this oxidation breached the carbonaceous blanket and extended to the premining, erosion surface. West of the orebodies, this alteration was a stratiform band in the siltstone just above the jasperoid. Contacts with overlying carbonaceous siltstone were discordant and generally concave downward. These contacts were marked by a pyrite-depleted transition zone usually 2 to 3 m wide in which organic matter had undergone incipient oxidation (Ilchik et al., 1986). Alunite ± barite veins present in the completely oxidized areas extended into these transition zones but were not present elsewhere in carbonaceous siltstone. The maroon, hematite-bearing oxidation in calcareous rocks was found adjacent to alunite-bearing oxidation. It was most prominent along minor faults in the area between the orebodies and the Vantage fault (Fig. 6A and B). Along the Vantage fault, oxidation penetrated up to 5 m into the Chainman Shale.

Weathering-related oxidation was present as a 5- to 20-m-thick zone in calcareous siltstone below the premining surface and, in deeper parts of the orebodies, was found adjacent to through-going fractures that extend from the surface (Fig. 5). Deep weathering generally occupied areas near the periphery of the orebodies or formed a thin band between carbonaceous rocks and alunite-bearing oxidation (Fig. 6A and B). Presumably this distribution was due to the destruction of sulfides and organic matter in the central portions of the orebodies prior to weathering. Contacts between weathered and carbonaceous rocks were marked by a gradual decrease in the abundance of organic matter over a distance of several meters. In other areas of the Vantage basin, most notably near its northwest corner, weathering has oxidized the entire Pilot Shale section.

Metal Distribution and Relationships to Alteration

Geometry and distribution

The economic orebodies in the Vantage basin were compact, individual pods containing ~1 to 2.5 million metric tons of ore at a cutoff grade of 1 ppm Au. Mineralization in the Vantage I, II, and III orebodies was continuous within each orebody, and virtually no subore-grade material was intermixed with ore. These orebodies were roughly hemispherical or bell-shaped, up to 75 m thick, and had nearly flat, stratiform bottoms (Fig. 8). The base of the ore was in jasperoid

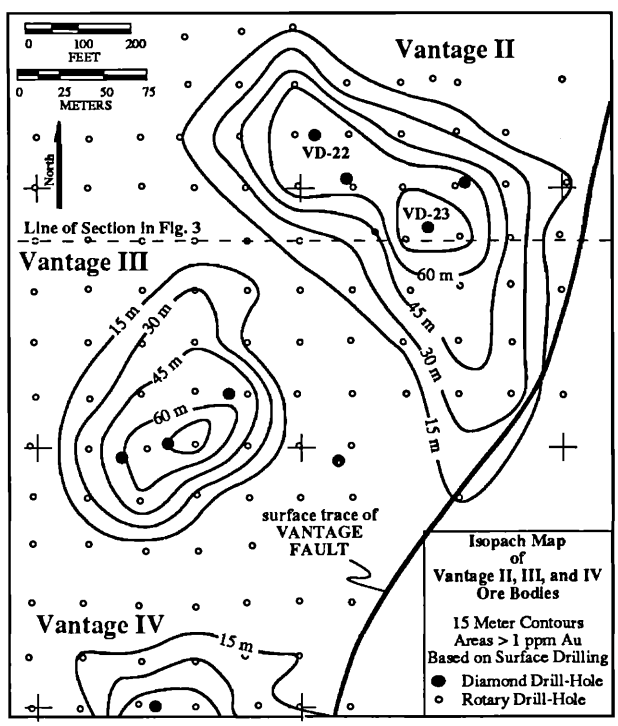

FIG. 8. Isopach map of ore thickness for Vantage II, III, and northern portion of IV. Data are from exploration rotary drill holes sampled over 5-ft intervals. All ore is in the footwall of the Vantage fault.

several meters above the contact with unreplaced limestone (Fig. 5). Subore-grade Au content extended to the limestone footwall but did not continue into fresh limestone. Vantage I and III were nearly circular in plan and 120 to 150 m in diameter. Vantage II, 120 × 270 m in plan, was elongated along a northwesterly trend, except near the Vantage fault, where it paralleled the fault.

Gold grades within these orebodies were crudely concentric (Fig. 6A and B). The highest grades were hosted by the Pilot Shale in the center of each deposit. Grade decreased outward from these high-grade centers and dropped abruptly from >3 ppm to <1 ppm Au over distances of 5 m or less at the ore-waste boundary. This boundary was generally coincident with the edge of decalcification and silicification. However, silicification was often spatially more extensive than ore, particularly near the Devils Gate Limestone-Pilot Shale contact. In other cases, ore grade extended up to 5 m across the silicification contact into dedolomitized, calcareous siltstone. Thus, assay data were the only reliable means to determine the ore-waste boundary.

Low-grade prospects in the district are typified by Vantage IV, the southernmost orebody of the Vantage deposit. These prospects tend to be irregular and more sheetlike in shape. Ore-grade material is confined to a narrow zone along the Devils Gate Limestone-Pilot Shale contact and is interfingered with altered, subore-grade material.

Alteration associations

Metal contents of the various alteration types in and around the Vantage orebodies showed systematic variations that were related to protolith and intensity of oxidation (Table 5). The Pilot Shale was the preferred host for precious metal mineralization over the Devils Gate jasperoids. Metals were redistributed during each period of oxidation, but the redistribution was much more extensive during the early alunite-producing event. Nearly all Au mineralization was hosted in carbonaceous siltstone, alunite-bearing oxidized siltstone, weathered noncalcareous siltstone, or jasperoid. The metal contents of the various calcareous siltstones and limestone were generally insignificant and are not discussed further. Gold and silver data for diamond drill holes which emphasize these relationships are shown in Figure 9.

Carbonaceous siltstone had the highest and most consistent content of Au (up to 25 ppm in blast holes), Ag, As, and Sb of all alteration types. Visible Au was not found in any samples of this ore type, in spite of a search of over one hundred polished sections. The Ag/Au ratio averaged 1.1. Arsenic contents ranged up to 5,000 ppm, and Sb in samples without quartz-kaolinite-stibnite veins was as high as 700 ppm. Mercury content determined on samples collected during the development stage of mining contained up to 4 ppm Hg, but the Hg content was generally less than 0.5 ppm for all rock types (unpub. company reports). Because of its general low abundance, Hg was not determined for samples in this study. Base metal content showed little difference from unaltered samples. Metal contents of carbonaceous ore were relatively constant over distances of tens of meters (Fig. 9). Grade changed rapidly only near contacts with alunite-bearing oxidized ore or near the edges of the orebodies. Gold content did not appear to be tied directly to the presence of quartz-kaolinite-stibnite veins because unveined samples were generally as

TABLE 5. Assay Data by Alteration Type

Alteration type[1]	Au[2] (ppm)	Ag/Au[2,3]	As[4] (ppm)	Sb[4] (ppm)	Cu[5] (ppm)	Pb[5] (ppm)	Zn[5] (ppm)	Number of analyses[6]	Percentage of tonnage[7]
Unaltered[8]	<0.005		40	10	25	27	117	19	
CCSl[9]	0.65	1.1	570	25	24	18	77	57	1–3
CSl	6.85	1.1	1010	110	29	20	160	160	5–45
OISl	4.50	0.4	760	50	30	21	83	175	30–50
OcSl	6.60	0.9	865	30	36	22	161	61	5–25
CaSl	1.15	0.1	410	35	na	na	na	36	1–3
Limestone	0.11	4.0	35	25	na	na	na	53	
Jasperoid	2.00	0.6	280	160	na	na	na	108	20

[1] Abbreviations as in Table 2, na = not available

[2] By fire assay or atomic absorption; detection limits: for Au = 0.07 ppm, for Ag = 0.3 ppm

[3] Calculated from average Au and Ag values for each rock type; assay pairs for individual samples display a wide variance, particularly for samples near detection limits, that results in unrepresentative averages

[4] By atomic absorption; detection limits: for As = 1 ppm, for Sb = 0.1 ppm

[5] XRF data, average of ~15 analyses per alteration type

[6] As and Sb data available for approximately one-half of the samples

[7] For individual orebodies; oxidized ore types predominate in Vantage I and decrease to Vantage III

[8] Samples from WSR-32 (Fig. 2); analyses by neutron activation, all others as indicated

[9] Samples collected within 150 m of orebodies

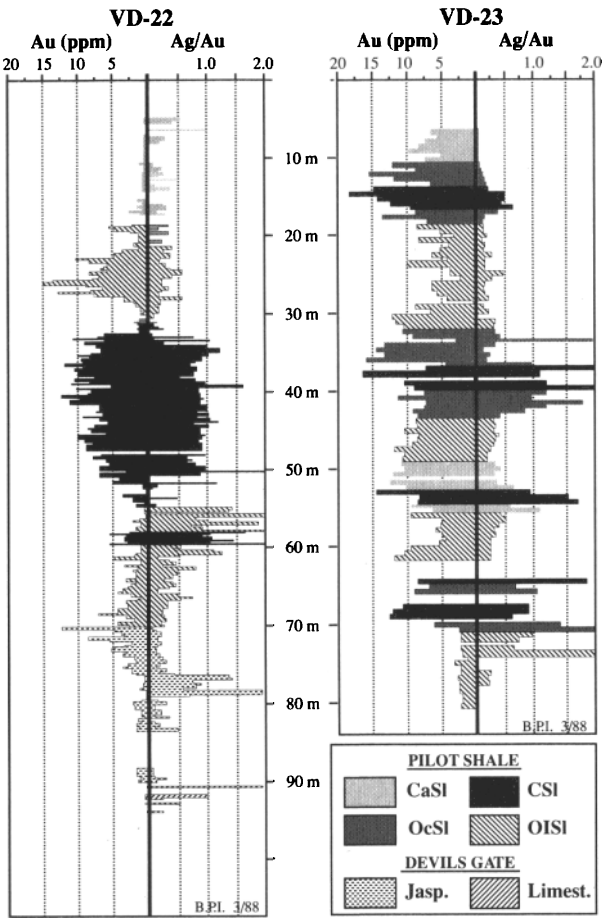

FIG. 9. Alteration logs for diamond drill holes VD-22 and VD-23 from Vantage II showing grade vs. alteration relationships. VD-22 was assayed on 1-ft intervals; VD-23 assayed on 2-ft intervals. Blank areas indicate no data. See Figure 8 for drill hole locations.

high in grade as nearby, highly veined samples. This and the lack of visible Au indicate that Au was truly disseminated in the carbonaceous ore.

Jasperoid had the lowest grade and was the most inconsistently mineralized ore type (Table 5). Gold grades in jasperoid were commonly less than one-third of the value in nearby carbonaceous ore (Fig. 9), and much less than half of the jasperoid in the vicinity of the Vantage deposits was ore. However, low-grade Au mineralization (≤0.5 ppm) was persistent throughout the unit. Silver and arsenic grades were also less than ~25 percent of that found in carbonaceous ore but Sb was higher. Quartz-stibnite veins were present in jasperoid but did not correlate spatially with Au grade as was the case for carbonaceous ore.

Alunite-bearing oxidized ore averaged about 30 percent less Au and As and less than half the Ag and Sb of carbonaceous ore. A systematic decline of Au and Ag grades was seen in carbonaceous ore as these oxidation contacts were approached, and local minima in Au and Ag concentrations often occurred at this contact (Fig. 9). Grades of less than 1 ppm Au (i.e., <10% of maximum value in adjacent carbonaceous intervals) were found for several meters across these contacts. Within the oxidized zones, the Au content approached that of carbonaceous ore, but detailed sampling often revealed erratic fluctuations indicative of a nugget effect. Macroscopic gold was relatively common in oxide ore and was generally found mantling vein quartz. Metallurgical tests indicated that approximately 15 percent of the Au in this ore was recoverable by gravitational means (Klessig, 1984). This change in the physical character of Au and the decreases in Au, Ag, As, and Sb indicate that remobilization of metals occurred during this period of oxidation. Gold appears to have moved only relatively short distances before reprecipitation (a few m to a few tens of m), while the more mobile elements Ag, Sb, and As were highly depleted (Table 5) or almost entirely removed.

In contrast to the earlier oxidation, weathering produced only minor decreases in Au, Ag/Au ratio, and As for this ore type relative to carbonaceous ore (Table 5). Antimony, however, was markedly lower than in other ore types. Two possible explanations for these data are that leaching of Sb occurred during weathering, and/or the protoliths of this ore had lower Sb grades prior to weathering than the remaining carbonaceous ore. The latter explanation is favored, because weathering generally affected material near the periphery of the deposits. Other data indicate that Sb contents were lower in these areas prior to weathering.

Stable Isotopes

Carbon, oxygen, and sulfur isotope compositions were determined on mineral separates and whole rocks selected from the various alteration assemblages. Background data from unaltered samples were acquired from samples used by Ilchik et al. (1986) in their study to establish background levels for the maturity of organic matter (drill hole WSR-32, Fig. 2). Gases for analysis were prepared using standard techniques. Carbonate CO_2 was extracted from 10- to 40-mg-size samples by reaction with 100 percent phosphoric acid at 25°C overnight in evacuated tubes. Silicate oxygen was liberated by reaction of 10- to 15-mg-size samples with ClF_3 at 600°C overnight in evacuated nickel metal vessels. The oxygen gas produced was converted to CO_2 by reaction with graphite in the presence of a platinum catalyst. Sulfide sulfur was liberated by digestion of sulfides in aqua regia in the presence of Br_2 to prevent the loss of sulfur as H_2S. Aqueous sulfate was precipitated as $BaSO_4$ by the addition of $BaCl_2$. Naturally occurring and syn-

thetic sulfates were thermally decomposed under vacuum to yield SO_2. Isotopic analyses were made using standard isotope-ratio mass spectrometry; data are reported in per mil using the δ notation. Carbon values are reported relative to PDB, oxygen values relative to SMOW, and sulfur values relative to Canyon Diablo troilite. Reproducibility for replicate analyses was near 0.1 per mil for $\delta^{18}O$ and $\delta^{13}C$ values and 0.5 per mil for $\delta^{34}S$ values.

Carbonates

Whole-rock carbonates showed a progressive shift in isotopic compositions to lower $\delta^{18}O$ and higher $\delta^{13}C$ values that correlates with replacement of dolomite by calcite (Fig. 10). Carbon and oxygen in four unaltered Pilot Shale samples average −1.3 per mil and 24.4 per mil, respectively; in Devils Gate Limestone these values are 0.7 per mil and 23.7 per mil. These values are typical for Devonian carbonates (Veizer and Hoefs, 1976). Alteration produced shifts of up to approximately 3 per mil in $\delta^{13}C$ values to 3.1 per mil and as much as −12 per mil in $\delta^{18}O$ values to 12.7 per mil. Significant enrichment in ^{13}C occurred only in those samples most depleted in ^{18}O (i.e., those closest to the orebodies), but decreases of several per mil in $\delta^{18}O$ values were found in samples collected 250 m from the orebodies. Vein calcites show similar but more extreme enrichments in ^{13}C and depletions in ^{18}O relative to unaltered whole rocks (Fig. 10). Values as high as 3.1 per mil for $\delta^{13}C$ and as low as 3.8 per mil for $\delta^{18}O$ were measured on vein calcite. Isotopic shifts in altered whole rocks appear to be the result of mixing between unaltered, indigenous CO_3^{-2} and a hydrothermal component represented by the vein calcite.

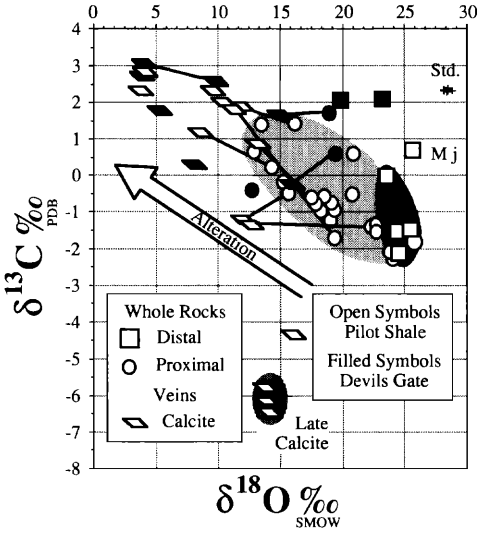

FIG. 10. Oxygen and carbon isotope data for carbonates from unaltered and calcareous carbonaceous siltstone samples. Lines connect calcite vein-whole rock pairs.

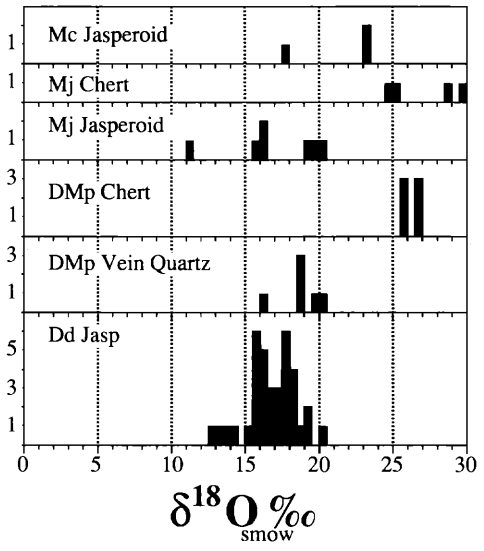

FIG. 11. Oxygen isotope data for jasperoids, cherts, and vein quartz presented by stratigraphic position.

Weathering-related, late calcite was isotopically lighter in $\delta^{13}C$ values and generally heavier in $\delta^{18}O$ values than hydrothermal vein calcite. Three samples yielded values for $\delta^{13}C$ of −5.8 to −6.5 per mil, and for $\delta^{18}O$ of 13.9 to 14.1 per mil (Fig. 10). These values are consistent with a low-temperature origin (O'Neil et al., 1969; Ohmoto and Rye, 1979).

Silicate oxygen

Oxygen isotope compositions were determined for jasperoids, vein quartz, and cherts in the district (Fig. 11). $\delta^{18}O$ values for Devils Gate jasperoids from the Vantage area varied between 15.9 and 18.2 per mil, and one sample from the Horseshoe prospect had a composition of 16.2 per mil. Jasperoids after Joana Limestone yielded similar values that varied from 15.6 to 20.2 per mil. Jasperoid after Chainman Limestone from near Horsehoe varied from 17.7 to 23.2 per mil. Isotopic compositions of vein quartz in Pilot Shale overlapped those for the jasperoids and varied from 16.1 to 20.1 per mil.

Cherts from the Pilot Shale and Joana Limestone had $\delta^{18}O$ compositions between 24.8 and 29.8 per mil. Devonian and Mississippian cherts generally have isotopic compositions that vary between 26 and 34 per mil (Knauth and Lowe, 1978). Many of the chert samples from the Joana Limestone were intimately intergrown with jasperoid, and the light values indicated for the chert probably resulted from contamination by intergrown jasperoid.

Sulfur

Data for epigenetic sulfur from the Au mineralization stage of alteration were acquired on whole rocks, stibnite, orpiment, and realgar (Fig. 12). Background data was also acquired for comparison with mineralized samples. Unaltered whole-rock values ranged from −4.1 to +4.5 per mil and averaged ~0.8 per mil. These values represent the $\delta^{34}S$ composition of diagenetic pyrite, the only premineralization sulfide. Altered whole rocks were enriched in ^{34}S relative to background and gave values as high as 11 per mil. The utility of whole-rock samples is equivocal, however, because they contained a mixture of epigenetic sulfides and diagenetic pyrite. Mineral separates of stibnite, orpiment, and realgar better represent epigenetic sulfur. The $\delta^{34}S$ values of ten stibnite samples varied from 5.5 to 10 per mil, four orpiment samples varied from 2.5 to 12.3 per mil, and one realgar sample yielded 14.4 per mil.

Barite from the district was subdivided into two groups based on habit: disseminated, and veins generally associated with alunite. Disseminated barite was found exclusively in jasperoid and consisted of isolated crystals, aggregates, or bedding parallel bands that were unrelated to fractures. Vein barite occurred as open-space fillings in fractures in oxidized siltstone, jasperoid, and rarely carbonaceous siltstone. Disseminated barite was isotopically heavy and varied from 25.9 to 47.1 per mil; most samples were heavier than 33 per mil (Fig. 12). Most samples of vein barite were isotopically lighter than the disseminated variety and generally varied between 21.0 and 29.2 per mil. Two samples from carbonaceous siltstone near the oxidation contact were, however, significantly heavier.

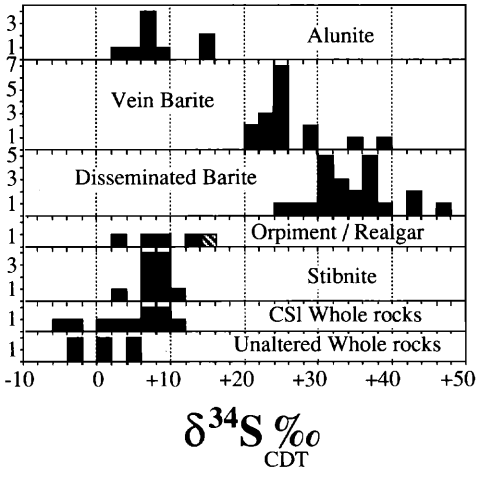

FIG. 12. Sulfur isotope data for various minerals and alteration types.

These samples had $\delta^{34}S$ values of 34.2 and 39.4 per mil.

Although vein barite clearly was introduced late in the history of the deposits, the origin of the disseminated barite is open to speculation. The habit of this barite suggests that it was inherited from unaltered Devils Gate Limestone. This assertion is supported by the isotopic differences from the vein barite, the fact that an early, silicification-related barite was not found in quartz-kaolinite-stibnite veins, and that barite is a common constituent in Devonian carbonates of the Great Basin (Papke, 1984). Sulfates generally have a composition that is approximately 1 per mil heavier than coexisting aqueous sulfate (Ohmoto and Rye, 1979). Upper Devonian seawater varied widely in $\delta^{34}S$ values (~23–32‰, Claypool et al., 1980), and the heavy values reported here are similar to Devonian barite nodules in the Appalachian basin Valley and Ridge province (Nuelle and Shelton, 1986) and to Silurian barite from central Nevada (Rye et al., 1978). Thus, a sedimentary or diagenetic origin rather than a hydrothermal origin is preferred for this barite.

Seven alunite samples examined had isotopic compositions of 3.8 to 13.5 per mil for $\delta^{34}S$ (Fig. 12). These values are strongly depleted relative to coexisting vein barite.

Discussion

Evolution of depositional environment: The temperature and pressure of formation for the Vantage deposits are weakly constrained. Unfortunately, fluid inclusions, although abundant, were generally too small for microthermometry. A few inclusions in calcite yielded homogenization temperatures of 200° to 230°C. If it is assumed that vein barite and stibnite were in isotopic equilibrium, then $\delta^{34}S$ data indicate temperatures of 190° to 250°C. These temperatures are consistent with the absence of mineralogic changes to the siliciclastic portion of the siltstone and is in line with data for the ore stage at Carlin (Radtke et al., 1980). Thus, 220° ± 30°C probably represents the temperature of formation. Erosion of the upper levels of Vantage I and II and the lack of explosion-related alteration indicate that the deposits did not form at the surface. Minimum depths of formation are suggested by phase relations visible in fluid inclusions. Relatively constant proportions of vapor and liquid in the inclusions indicate that the fluid did not boil. A minimum pressure of 16 bars at 200°C is required to prevent boiling, or a depth of approximately 600 m at a hydrostatic gradient (calculated via SUPCRT compute code, Helgeson et al., 1978).

The preservation of organic matter and sulfides during Au deposition indicate that the ore fluid was

reduced (i.e., $H_2S > \Sigma SO_4$). This suggests that Au was transported as a bisulfide complex (Seward, 1973). The lack of barite associated with silicification is compatible with a low oxidation state during Au deposition. The subsequent destruction of sulfides and organic matter, the production of alunite and vein barite, and the lack of Au associated with this stage of alteration indicate that the system evolved to a barren, oxidized sulfur-dominated one, if these changes were produced by the same system as the Au mineralization. This suggests that the sulfur isotope compositions of epigenetic sulfides and barite may represent equilibrium between sulfide and sulfate in the ore fluid. As a lower activity of oxidized sulfur is required to precipitate barite than to form alunite, it is rational that formation of barite would occur prior to the formation of alunite.

The existence of both alunite-bearing and jarosite-bearing oxidation assemblages formed from the same protolith indicates that the physical and/or chemical conditions that produced these assemblages were different. The spatial distribution of the jarosite-bearing assemblage clearly links it to weathering. The origin of the alunite-bearing oxidation in the deposits, though, is not completely understood. This oxidation could be simply a more intense form of weathering that resulted in the complete destruction of organic matter and sulfides. A hydrothermal origin, however, is preferred for alunite-bearing oxidation. Alunite-bearing oxidation was spatially associated with silicification and centered on the same conduits used by Au-bearing fluids. Contacts with overlying carbonaceous siltstone were concave downward and suggested an outward progression of oxidation from these conduits. In contrast, the deeper extents of weathering-related oxidation were directly associated with high-angle fractures that reached the erosion surface. This spatial distribution provides a link between the alunite-bearing oxidation and the hydrothermal Au mineralization event.

Sulfur isotopes of alunite and barite provide a second link between the alunite-bearing oxidation and the Au deposition event. Alunite and vein barite were closely associated spatially and appear to have been nearly contemporaneous, although alunite was always slightly later. Alunite $\delta^{34}S$ values are similar to the whole-rock sulfur values for carbonaceous ore. This suggests that alunite sulfur was derived in situ by oxidation of preexisting sulfides in the deposit. In contrast, sulfur in vein barite was up to 20 per mil heavier than coexisting alunite and was highly fractionated relative to the average sulfur composition of the deposits. It is unlikely that this sulfur was derived directly from oxidation of sulfides in the deposits (Ohmoto and Rye, 1979); thus, it was probably introduced hydrothermally as aqueous sulfate.

Chemical evolution of alteration: The geological and geochemical features of the Vantage deposits indicate that mineralization and alteration resulted from a two-stage hydrothermal process which was followed by a period of weathering.

Silicification and decalcification occurred early in formation of the deposits and were accompanied by precious metal mineralization. Petrographic observations indicate that the early, replacement-type alteration was essentially a coupled solubility reaction for calcite and quartz. The solubilities can be represented, conserving volume of the solids, by the reaction:

$$0.976\ SiO_{2(aq)} + CaCO_{3(calcite)} = Ca^{+2} + CO_3^{-2} + 0.976\ SiO_{2(quartz)}, \quad (1)$$

where dissolution of carbonate provides the space needed for quartz precipitation. Calcium removed from the silicified zones was deposited as calcite in veins and as a replacement of dolomite in adjacent areas. Volume-conservative replacement of dolomite can be represented by the reaction:

$$0.475Ca^{+2} + 1.05(CaMg)CO_3 = 0.525Mg^{+2} + 0.05CO_3^{-2} + CaCO_3. \quad (2)$$

It must be emphasized that the degree of coupling of these solubilities is not well known, but the reactions are consistent with field and petrographic observations.

Boundaries for Au mineralization with subore-grade material were generally sharp contacts often less than a meter wide. This indicates that precipitation mechanisms for Au were efficient at removing the metal from solution. The general coincidences of the ore boundaries with the decalcification fronts indicates that decalcification-silicification and Au deposition may be linked. However, Au showed a marked preference for the siltstone over altered limestone, in spite of the similar alteration in both units. The reasons for this preference are unclear. It could be that organic matter acted as a reductant, or that the presence of illite in the siltstone provided surface area to catalyze Au precipitation (Bakken et al., 1989). The depositional mechanisms are not well understood and deserving of further study.

Oxidation redistributed metals and masked many features associated with the introduction of Au. Oxidation of the illite + pyrite-bearing assemblage (i.e., carbonaceous siltstone) to produce the alunite and hematite present in the early oxidation assemblage can be represented by the reaction:

$$2K_{0.5}Al_{2.5}Si_{3.5}O_{10}(OH)_2 + FeS_2 + 3H_2O + 3.75O_2 = KAl_3(SO_4)_2(OH)_6 + Al_2Si_2O_5(OH)_4 + 5SiO_2 + 0.5Fe_2O_3. \quad (3)$$

Analogously, formation of jarosite during late oxidation is given by:

$$2K_{0.5}Al_{2.5}Si_{3.5}O_{10}(OH)_2 + 3FeS_2 + 10H_2O + 11.25O_2 = KFe_3(SO_4)_2(OH)_6 + 2.5Al_2Si_2O_5(OH)_4 + 2SiO_2 + 4HSO_4^- + 4H^+. \quad (4)$$

A low pH is require to stabilize alunite or jarosite over the illite-bearing assemblage (Hemley et al., 1969); thus, reactions (3) and (4) are appropriate only for noncalcareous rocks. In calcareous rocks, illite would be stable and oxidation would form either hematite (early oxidation peripheral to alunite-bearing oxidation) or goethite (weathering) from pyrite.

The composition of the Pilot Shale places mass balance constraints on the extent to which reactions (3) and (4) can proceed and appear to account for the textural differences between the two assemblages. Carbonaceous siltstone contains roughly 0.1 mol S/100 g (3 wt %) and 0.1 mol illite/100 g (38 wt %). Oxidation via reaction (3) consumes S and illite in equal proportions and, if carried to completion, produces 0.05 mol alunite/100 g (~20 g) and 0.25 mol quartz/100 g (~15 g). In contrast, if all the S reacted via reaction (4), the availability of pyrite limits the extent to which the reaction can proceed. Given the abundance of pyrite in the Pilot Shale, reaction (4) can produce 0.017 mole jarosite/100 g (~8 g) and only 0.033 mole quartz/100 g (~2 g). The amount of illite is reduced by 0.033 mole/100 g (~12 g), but a nearly equal mass of kaolinite is produced. The silica released in reaction (3), if precipitated as a cement, would produce the induration associated with the alunite-bearing oxidation; the conversion of illite to kaolinite during production of jarosite via reaction (4) would produce only minor textural modifications.

Sources of fluids and sulfur: Estimates of the oxygen isotope composition of the hydrothermal fluids can be made at an assumed temperature from the isotopic compositions of jasperoid, vein quartz, and carbonate. The high variability of $\delta^{18}O$ values for vein calcite, however, indicates that the isotopic composition and/or temperature of the fluid varied rapidly as it moved through the area of the deposits. Therefore, a value based on quartz seems most likely to reflect the composition of the incoming fluid. Fluid in equilibrium with Devils Gate jasperoid and vein quartz (avg composition = 17.1 ± 1.9‰ for 38 samples) at ~200°C would have a $\delta^{18}O$ value of 3.9 ± 1.0 (Matsuhisa et al., 1979). This fluid composition is in the range of Tertiary meteoric waters in the Great Basin ($\delta^{18}O \sim -12$‰; Sheppard, 1986) that have exchanged with relatively heavy sediments ($\delta^{18}O > 12$‰), and is similar to $\delta^{18}O$ values calculated for other Carlin-type deposits where δD values support this origin (Rye et al., 1974; Radtke et al., 1980; Hofstra et al., 1988). Without δD values there is uncertainty, but these data are compatible with the ore fluid being primarily an evolved meteoric water.

A regional study of the oxygen isotope compositions of jasperoids in the eastern Great Basin (Holland et al., 1988) reports that jasperoids associated with Au deposits generally have $\delta^{18}O$ values of 8 to 20 per mil, whereas barren jasperoids have lighter oxygen. All the values reported here fall within the productive range regardless of their proximity to ore or stratigraphic position, but Joana and Chainman jasperoids do not in general host even subore-grade mineralization. The similarity in isotopic compositions between productive and barren jasperoids in the district, however, indicates that all the jasperoids formed by similar processes. Therefore, the data from Alligator Ridge indicate that $\delta^{18}O$ data for jasperoids must be viewed as a district scale rather than as a deposit scale exploration tool.

The source of epigenetic sulfur can be inferred from sulfur isotope data for hydrothermal sulfides. Assuming that little fractionation occurred between source and aqueous sulfide (Ohmoto and Rye, 1979), the $\delta^{34}S$ data are compatible with a diagenetic pyrite source. The requirements for an external source of components preclude the Pilot and Chainman Shales as the sulfur sources. Therefore, the most likely source for sulfur of this composition are Cambrian shales and siltstones (Nolan et al., 1956). By extension, these units may also be the source for other materials in the deposits. Based on stratigraphic considerations this suggests that fluid circulation was from a depth of 3 km or more.

Fluid migration paths: The distributions of alteration, Au grades, and ore thickness presumably reflect the paleohydrology of the ore forming system. Hydrothermal fluids ascended through massive carbonate rocks from depth up the Vantage fault. Near the level of the deposits the low permeability of the Chainman Shale impeded fluid flow along the fault and shifted flow to smaller structures in the brittle, uppermost Devils Gate Limestone (Ilchik et al., 1986, fig. 13). The central, discordant silicification and alunite-bearing oxidation that formed the high-grade core of each deposit occurred over fractures which acted as local conduits for ore fluids. At the contact with the Pilot Shale, flow became intergranular and predominantly lateral. The peripheral, more stratiform alteration was probably due to enhanced permeability along the siltstone-limestone contact. Alteration in the Chainman Shale mudstones east of the Vantage fault was restricted by their low permeability.

Preservation of fine textural features indicates that hydrothermal activity was generally a passive, nondisruptive process, rather than a violent one. An explosive origin, however, has been suggested for some

of the breccias in the deposits (Tapper, 1986), but a tectonic origin is more likely. The Pilot Shale is a relatively incompetent lithology and is susceptible to mechanical disaggregation, especially prior to induration associated with oxidation. Most of the breccias (see section on structure) have linear map patterns, and minor offsets can be documented across the breccia zones. Thus, minor fault movement and/or collapse would make spectacular, but spatially limited, breccias.

Comparison with other deposits: As a group the Carlin-type sediment-hosted precious metal deposits show a remarkable consistency in their geological and geochemical features. These similarities should be stressed in any general model that seeks to account for the formation of the deposits, whereas local controls should be examined to account for the differences between deposits. Several compilations of data for the deposits have been published (Tooker, 1985; Bagby and Berger, 1985); thus, this discussion is not intended to provide a comprehensive review of these other deposits but rather to compare the Alligator Ridge-Bald Mountain district with other areas.

Carlin-type deposits occur throughout much of the Great Basin. The occurrence of multiple orebodies as in the Alligator Ridge-Bald Mountain district is a feature common to many other districts and indicates that the deposits are related to some larger scale processes. Intrusive rocks are not always present in the vicinity of the deposits, thus a heat source for the hydrothermal fluids is not always readily apparent. This may be due to the large size inferred for the systems (Rye, 1985; Rose and Kuehn, 1987).

The metal association of Au, As, and Sb is common to all Carlin-type deposits, and the lack of Hg is not unusual (Bagby and Berger, 1985). The average Ag/Au ratio of 1.1 is high for this type of deposit, but considering the low metal content (in absolute terms), minor changes in the content of either metal would cause large fluctuations in this ratio. Weak enrichment in Cu, Pb, Zn, W, and F are reported for some deposits, whereas many deposits, including Vantage, show no enrichment over background values.

The alteration and paragenesis for the Vantage deposits are similar in most ways to those given for other Carlin-type deposits. The strongest similarities with the larger deposits are in the host rocks and in the carbonate replacement that accompanies Au mineralization. Carbonaceous, silty carbonate rocks are the host rocks at the majority of the deposits. Where other lithologies also host mineralization, they generally are of secondary economic importance. Silicification at other deposits is not always as complete as it is in the Vantage deposits. At Carlin (Bakken and Einaudi, 1986; Radtke et al., 1980) and Jerritt Canyon (Birak and Hawkins, 1985) up to 25 percent carbonate, mainly dolomite, remains in the ores. Unaltered host rocks for these deposits and Vantage contain roughly the same amount of carbonate, so this does not account for the differing degrees of decalcification. In addition, calcite replacement of dolomite peripheral to ore has not been reported at any other deposits.

Bagby and Berger (1985) reviewed the characteristics of 31 deposits and concluded that intensity of silicification could be used to subdivide sediment-hosted precious metal deposits into two categories. Deposits with large, well-developed jasperoids were deemed jasperoidal deposits, and those with relatively little apparent silicification were deemed Carlin-type. Petrographic data from the Vantage deposits indicate that the carbonate content of the host rock limits the amount of silica that can be added during alteration. Thus, this classification scheme may simply reflect differences in host-rock lithologies and is not an indication of differences in the hydrothermal processes that resulted in the deposits.

Argillization is reported at several deposits (Bagby and Berger, 1985). Argillization is not important at Vantage because of the lack of feldspar in the host rocks. Decalcification, however, makes the Pilot Shale friable and imparts an appearance of argillic alteration to the siltstone. Host rocks for other deposits, in general, also contain large amounts of phyllosilicates and lack feldspar. Thus, it is possible that primary clays have been mistaken for alteration products. This seems to have been the case at Jerritt Canyon where careful clay petrography shows that phyllosilicates, which originally were thought to be hydrothermal (Birak and Hawkins, 1985), are of detrital origin (D. J. Birak, pers. commun., 1988).

Oxidation in Carlin-type deposits spans a range from minor to extensive. Only weathering-related oxidation, which conforms to the premining topography, is present at Jerritt Canyon (Birak, 1986). At the Carlin deposit, extensive deep oxidation was present (Radtke et al., 1980) and fluid inclusion data were used to suggest that this oxidation was the result of late-stage boiling of hydrothermal fluids. Although alunite was not reported at Carlin, a few km south at the Gold Quarry deposit alunite is present to a depth of several hundred feet (C. Ekburg, pers. commun., 1988). Thus, the oxidation states of the ore fluids for several deposits (e.g., Carlin and Vantage) seem to have varied from an early, relatively reduced state to a later, oxidized state. This may not be the case at most deposits, however, as alunite-bearing alteration appears to be the exception rather than the rule. Also, it appears that there is no single cause for late-stage oxidation, as there was no evidence for boiling at the Vantage deposits.

Conclusions

The Alligator Ridge-Bald Mountain district contains multiple Carlin-type sediment-hosted gold deposits

and numerous areas of related subore-grade alteration. The widespread nature of mineralization is similar to other districts and suggests that the processes that lead to the formation of the deposits is related to regional-scale developments. However, the exact links between regional geologic development and the processes of mineralization remain obscure.

The Vantage deposits are representative examples of Carlin-type gold deposits that were relatively uncomplicated by extraneous geologic processes. Gold mineralization was preferentially hosted in the silty, carbonaceous rocks of the Pilot Shale over the micrites of the Devils Gate Limestone. Silver, arsenic, and antimony accompany gold. Alteration most closely associated with Au mineralization was the replacement of host-rock carbonate with quartz. This alteration was nearly coincident with the ore zones. A zone of calcite replacement of dolomite was present in the areas peripheral to Au mineralization. This replacement was accompanied by shifts in the isotopic compositions of the carbonate and may contain anomalous concentrations of As. A period of intense oxidation followed Au mineralization. At this time all sulfides and organic matter in much of the deposit were destroyed and alunite ± barite veins were formed. It is thought that this oxidation represents the waning stages of hydrothermal activity.

Oxygen isotope data for carbonates, vein quartz, and jasperoid suggest that the ore fluid was dominated by highly evolved meteoric waters. Sulfur isotope data suggest that sulfur in the ore fluid was derived from sedimentary sulfides in lower stratigraphic horizons. Together, these data suggest that the ore fluid circulated to a depth of several kilometers in the crust to acquire its chemical and isotopic composition.

Stratigraphic and geologic data indicate that the Vantage deposits formed within a kilometer or so of the surface, but no evidence for surface emanations of the hydrothermal fluids was present. Fluids responsible for the formation of the deposits ascended to the ore horizon along a major fault zone. At the contact between the Pilot Shale and the Devils Gate Limestone fluid flow was dispersed into small fractures and pores of the Pilot and along the contact. The greater permeability, organic matter, or clay minerals of the Pilot Shale may account for its preference as the ore host. Chemical and fluid flow models of the system may help to illuminate the mechanisms involved in gold deposition.

Acknowledgments

This work was generously supported by B. P. Minerals America, who also granted access to mine data. A. P. Taylor, H. W. Schull, and S. M. Sutherland deserve particular acknowledgment for their continuing encouragement and support. P. J. Klessig provided some of the data for Figure 6. Numerous discussions with Mark D. Barton helped develop the ideas presented here. Review of this manuscript by C. E. Seedorff and two *Economic Geology* reviewers helped to refine the presentation. Stable isotope studies were partially supported by NSF EAR 86-07452 to M. D. Barton. I am grateful for K-Ar measurements, performed on a gratis basis, by Krueger Enterprises, Inc., Geochron Laboratories Division, Cambridge, Massachusetts, and by L. Pickthorn, U. S. Geological Survey, Menlo Park, CA. Early portions of this study were directed by G. H Brimhall.

February 28, October 11, 1989

REFERENCES

Ashley, R. P., and Silberman, M. L., 1976, Direct dating of mineralization at Goldfield, Nevada, by potassium-argon and fission-track methods: ECON. GEOL., v. 71, p. 904–924.

Bagby, W., and Berger, B. R., 1985, Geologic characteristics of sediment-hosted, disseminated precious-metal deposits in the western United States: Rev. Econ. Geology, v. 2, p. 169–202.

Bakken, B. M., and Einaudi, M. T., 1986, Spatial and temporal relation between wall rock alteration and gold mineralization, main pit, Carlin gold mine, Nevada, U.S.A., *in* Macdonald, A. J., ed., Gold '86: Willowdale, Ontario, Konsult Internat. Inc., p. 388–403.

Bakken, B. M., Hochella, M. F., Jr., Marshall, A. F., and Turner, A. M., 1989, High-resolution microscopy of gold in unoxidized ore from the Carlin mine, Nevada: ECON. GEOL., v. 84, p. 171–179.

Barton, M. D., in press, Cretaceous magmatism, mineralization and metamorphism in the east-central Great Basin: Geol. Soc. America Memoir 174.

Birak, D. J., 1986, Exploration and geologic development of the Jerritt Canyon gold deposits, Elko County, Nevada, U.S.A., *in* Macdonald, A. J., ed., Gold '86: Willowdale, Ontario, Konsult Internat. Inc., p. 488–496.

Birak, D. J., and Hawkins, R. J., 1985, The geology of the Enfield Bell mine and the Jerritt Canyon district, Elko County, Nevada: U. S. Geol. Survey Bull. 1646, p. 95–105.

Blake, J. W., 1964, Geology of the Bald Mountain intrusive, Ruby Mountains, Nevada: Brigham Young Univ. Geol. Studies, v. 11, p. 3–35.

Brew, D. A., 1971, Mississippian stratigraphy of the Diamond Peak area, Eureka County, Nevada: U. S. Geol. Survey Prof. Paper 661, 84 p.

Claypool, G. E., Holser, W. T., Kaplan, I. R., Sakai, H., and Zack, I., 1980, The age curves of sulfur and oxygen isotopes in marine sulfate and their mutual interpretation: Chem. Geology, v. 28, p. 199–260.

Cunningham, C. G., Jr., Rye, R. O., Steven, T. A., and Mehnert, H. H., 1984, Origin and exploration significance of replacement and vein-type alunite deposits in the Marysvale volcanic field, west central Utah: ECON. GEOL., v. 79, p. 50–71.

Gans, P. B., Mahood, G. A., and Schermer, E., 1989, Synextentional magmatism in the Basin and Range province; a case study from the eastern Great Basin: Geol. Soc. America Spec. Paper 233, 53 p.

Gutschick, R. C., and Rodriguez, J., 1979, Biostatigraphy of the Pilot Shale (Devonian-Mississippian) and contemporaneous strata in Utah, Nevada and Montana: Brigham Young Univ. Geol. Studies, v. 26, p. 37–63.

Hausen, D. M., and Kerr, P. F., 1968, Fine gold occurrence at Carlin, Nevada, *in* Ridge, J. D., ed., Ore deposits of the United States, 1933–1967 (Graton-Sales vol.): New York, Am. Inst. Mining Metall. Petroleum Engineers, v. 1, p. 908–940.

Helgeson, H. C., Delany, J. M., Nesbitt, H. W., and Bird, D. K.,

1978, Summary and critique of the thermodynamic properties of rock-forming minerals: Am. Jour. Sci., v. 278A, 229 p.

Hemley, J. J., Hostetler, P. B., Gude, A. J., and Mountjoy, W. T., 1969, Some stability relations of alunite: ECON. GEOL., v. 64, p. 599–612.

Hill, J. M., 1916, Notes on some mining districts in eastern Nevada: U. S. Geol. Survey Bull. 648, 214 p.

Hofstra, A. H., Northrop, H. R., Rye, R. O., Landis, G. P., and Birak, D. J., 1988, Origin of sediment-hosted disseminated gold deposits by fluid mixing—evidence from jasperoids in the Jerritt Canyon gold district, Nevada, U.S.A.: Geol. Soc. Australia Abstracts, no. 22, p. 284–289.

Holland, P. T., Beaty, D. W., and Snow, G. G., 1988, Comparative elemental and oxygen isotope geochemistry of jasperoid in the northern Great Basin: Evidence for distinctive fluid evolution in gold-producing hydrothermal systems: ECON. GEOL., v. 83, p. 1401–1423.

Hose, R. K., and Blake, M. C., Jr., 1976, Geology and mineral resources of White Pine County, Nevada, Pt. I: Nevada Bur. Mines Bull. 85, p. 1–35.

Ilchik, R. P., in press, Geology of the Vantage gold deposits, Alligator Ridge, Nevada, *in* Schafer, R. W., and Wilkinson, W. H., eds., Geology and ore deposits of the Great Basin symposium proceedings: Geol. Soc. Nevada.

Ilchik, R. P., Brimhall, G. H., and Schull, H. W., 1986, Hydrothermal maturation of indigenous organic matter at the Alligator Ridge gold deposits, Nevada: ECON. GEOL., v. 81, p. 113–130.

Klessig, P. J., 1984, History and geology of the Alligator Ridge gold mine, White Pine Co., Nevada: Arizona Geol. Soc. Digest, v. 15, p. 77–88.

Knauth, L. P., and Lowe, D. R., 1978, Oxygen isotope geochemistry of cherts from the Onverwacth Group (3.4 billion years), Transvaal South Africa, with implications for secular variations in the isotopic composition of cherts: Earth Planet. Sci. Letters, v. 41, p. 209–222.

Matsuhisa, Y., Goldsmith, J. R., and Clayton, R. N., 1979, Oxygen isotopic fractionation in the system quartz-albite-anorthite-water: Geochim. et Cosmochim. Acta, v. 43, p. 1131–1140.

Miller, E. L., Gans, P. B., Wright, J. E., and Sutter, J. F., 1988, Metamorphic history of the east-central Basin and Range province: Tectonic setting and relationship to magmatism, *in* Ernst, W. G., ed., Metamorphism and crustal evolution, western conterminous United States, (Rubey vol. VII): Englewood Cliffs, New Jersey, Prentice-Hall, p. 649–682.

Nolan, T. B., Merriam, C. W., and Williams, J. S., 1956, The stratigraphic section in the vicinity of Eureka, Nevada: U. S. Geol. Survey Prof. Paper 276, 77 p.

Nuelle, L. M., and Shelton, K. L., 1986, Geologic and geochemical evidence of possible bedded barite deposits in Devonian rocks of the valley and ridge province, Appalachian Mountains: ECON. GEOL., v. 81, p. 1408–1430.

Ohmoto, H., and Rye, R. O., 1979, Isotopes of sulfur and carbon, *in* Barnes, H. L., ed., Geochemistry of hydrothermal ore deposits, 2nd ed.: New York, Wiley Intersci., p. 509–567.

O'Neil, J. R., Clayton, R. N., and Mayeda, T. K., 1969, Oxygen isotope fractionation in divalent metal carbonates: Jour. Chem. Physics, v. 51, p. 5547–5558.

Papke, K. G., 1984, Barite in Nevada: Nevada Bur. Mines Bull. 85, 125 p.

Radtke, A. S., Rye, R. O., and Dickson, F. W., 1980, Geology and stable isotope studies of the Carlin gold deposit, Nevada: ECON. GEOL., v. 75, p. 641–672.

Rigby, J. K., 1960, Geology of the Buck Mountain—Bald Mountain area, southern Ruby Mountains, White Pine County, Nevada, *in* Guidebook to the geology of east-central Nevada: Intermountain Assoc. Petroleum Geologists and Eastern Nevada Geol. Soc. Ann. Field Conf., 11th, 1960, Salt Lake City, Utah, p. 173–180.

Rose, A. W., and Kuehn, C. A., 1987, Ore deposition from acidic CO_2-rich solutions at the Carlin gold deposits, Eureka County, Nevada [abs.]: Geol. Soc. America Abstracts with Programs, v. 19, p. 824.

Rye, R. O., 1985, A model for the formation of carbonate-hosted disseminated gold deposits based on geologic, fluid inclusion, geochemical, and stable isotope studies of the Carlin and Cortez deposits, Nevada: U. S. Geol. Survey Bull. 1646, p. 35–42.

Rye, R. O., Doe, B. R., and Wells, J. D., 1974, Stable isotope and lead isotope studies of the Cortez, Nevada, gold deposit and surrounding area: U. S. Geol. Survey Jour. Research, v. 2, p. 13–23.

Rye, R. O., Shawe, D. R., and Poole, F. G., 1978, Stable isotope studies of bedded barite at East Northumberland Canyon in Toquima Range, central Nevada: U. S. Geol. Survey Jour. Research, v. 6, p. 221–229.

Seward, T. M., 1973, Thiocomplexes of gold and the transport of gold in hydrothermal ore solutions: Geochim. et Cosmochim. Acta, v. 37, p. 379–399.

Sheppard, S. M. F., 1986, Characterization and isotopic variations in natural waters: Rev. Mineralogy, v. 16, p. 165–183.

Smith, R. M., 1976, Geology and mineral resources of White Pine County, Nevada, Pt. II: Nevada Bur. Mines Bull. 85, p. 35–105.

Stewart, J. H., 1980, Geology of Nevada: Nevada Bur. Mines Spec. Pub. 4, 136 p.

Tapper, C. J., 1986, Geology and genesis of the Alligator Ridge mine, White Pine County, Nevada: Nevada Bur. Mines Rept. 40, p. 85–103.

Thomas, P. R., and Boyle, E. H., Jr., 1986, Gold availability—world: A minerals availability appraisal: Washington, D. C., U. S. Bur. Mines, 87 p.

Tooker, E. W., 1985, Discussion of the disseminated-gold-ore-occurrence model, *in* Tooker, E. W., ed., Geologic characteristics of sediment- and volcanic-hosted disseminated gold deposits—search for an occurrence model: U. S. Geol. Survey Bull. 1646, p. 107–150.

Veizer, J., and Hoefs, J., 1976, The nature of O^{18}/O^{16} and C^{13}/C^{12} secular trends in sedimentary carbonate rocks: Geochim. et Cosmochim. Acta, v. 40, p. 1387–1395.

Wells, J. D., and Mullens, T. E., 1973, Gold-bearing Arsenian pyrite determined by microprobe analysis, Cortez and Carlin gold mines, Nevada: ECON. GEOL., v. 68, p. 187–201.

Woods, T. L., and Garrels, R. M., 1987, Thermodynamic values at low temperatures for natural inorganic materials: An uncritical summary: New York, Oxford Univ. Press, 242 p.